Available online at www.sciencedirect.com
ScienceDirect
Geomorphology 99 (2008) 150–170
GEOMORPHOLOGY
www.elsevier.com/locate/geomorph

A roughness-corrected index of relative bed stability for regional stream surveys

Philip R. Kaufmann [a,*], John M. Faustini [b], David P. Larsen [c], Mostafa A. Shirazi [a]

[a] *Western Ecology Division, National Health and Environmental Effects Laboratory, Office of Research and Development, U.S. Environmental Protection Agency, 200 SW 35th Street, Corvallis, OR 97333, USA*
[b] *Department of Fisheries and Wildlife, Oregon State University, c/o U.S. Environmental Protection Agency, 200 SW 35th Street, Corvallis, OR 97333, USA*
[c] *Pacific States Marine Fisheries Commission, c/o U.S. Environmental Protection Agency, 200 SW 35th Street, Corvallis, OR 97333, USA*

Received 21 April 2007; received in revised form 19 October 2007; accepted 22 October 2007
Available online 26 October 2007

Abstract

Quantitative regional assessments of streambed sedimentation and its likely causes are hampered because field investigations typically lack the requisite sample size, measurements, or precision for sound geomorphic and statistical interpretation. We adapted an index of relative bed stability (RBS) for data calculated from a national stream survey field protocol to enable general evaluation of bed stability and anthropogenic sedimentation in synoptic ecological surveys. RBS is the ratio of bed surface geometric mean particle diameter (D_{gm}) divided by estimated critical diameter (D_{cbf}) at bankfull flow, based on a modified Shield's criterion for incipient motion. Application of RBS to adequately depict bed stability in complex natural streams, however, has been limited because typical calculations of RBS do not explicitly account for reductions in bed shear stress that result from channel form roughness. We modified the index (RBS*) to incorporate the reduction in bed shear stress available for sediment transport that results from the hydraulic resistance of large wood and longitudinal irregularities in channel dimensions ("form roughness"). Based on dimensional analysis, we derived an adjustment to bankfull shear stress by multiplying the bankfull hydraulic radius (R_{bf}) by the one-third power of the ratio of particle-derived resistance to total hydraulic resistance $(C_p/C_t)^{1/3}$, where both resistances are empirically based calculations. We computed C_p using a Keulegan equation relating resistance to relative submergence of bed particles. We then derived an empirical equation to predict reach-scale hydraulic resistance C_t from thalweg mean depth, thalweg mean residual depth, and large wood volume based on field dye transit studies, in which total hydraulic resistance C_t was measured over a wide range of natural stream channel complexity, including manipulation of large wood volumes. We tested our estimates of C_t and RBS* by applying them to data from a summer low flow probability sample of 104 wadeable stream reaches in the Coastal Ecoregion of Oregon and Washington, USA. Stream discharges calculated using these C_t estimates compared favorably with velocity–area measurements of discharge during summer low flow, and with the range of 1 to 2-year recurrence floods (scaled by drainage area) at U.S.Geological Survey gauged sites in the same region. Log [RBS*] ranged from −4.2 to +0.98 in the survey region. D_{gm} ranged from silt to boulders, while estimated bankfull critical diameter, D^*_{cbf}, ranged from very fine gravel to large boulders. The median value of D^*_{cbf} (adjusted for form roughness influences) averaged 40% (inter quartile range 28 to 59%) of the unadjusted estimate D_{cbf}. Log[RBS*] was consistently negatively related to human disturbances likely to produce excess sediment inputs or hydrologic alteration. Log [RBS*] ranged from −1.9 to +0.5 in the streams within the lower quartile of human disturbance in their basin and riparian areas and was substantially lower (−4.2 to −1.1) in streams within the upper quartile of human disturbance. The synoptic survey methods and designs we used appear adequate to evaluate *regional* patterns in bed stability and sedimentation and their general relationship to human disturbances. Although the RBS concept also shows promise for evaluating sediment and bed stability in individual streams, our approach is relatively coarse, so site-specific assessments using these rapid field methods might prudently be confined to identifying severe cases of sedimentation or channel alteration. Greater confidence to discern subtle differences in site-specific assessments could be gained by calculating RBS* using more precise field measurements of channel slope, bed particle size and bankfull dimensions, and by refining our adjustments for energy loss from channel form roughness.
Published by Elsevier B.V.

Keywords: Rivers/streams; Sediment transport; Environmental indicators; Hydraulic resistance; Bedform roughness

* Corresponding author. Tel.: +1 541 754 4451; fax: +1 541 754 4716.
E-mail addresses: kaufmann.phil@epa.gov (P.R. Kaufmann), faustini.john@epa.gov (J.M. Faustini), larsen.phil@epa.gov (D.P. Larsen), shirazi.mostafa@epa.gov (M.A. Shirazi).

0169-555X/$ - see front matter. Published by Elsevier B.V.
doi:10.1016/j.geomorph.2007.10.007

1. Introduction

Routine state and regional habitat surveys commonly measure sediment size composition and other channel attributes to assess the extent and biological effects of anthropogenic sedimentation. However, their interpretations commonly fall short of discerning probable controls on stream bed particle size because they lack key measurements and a process-based analytical framework for interpreting sediment data. Detailed studies of watershed erosion and channel sediment transport can be undertaken to assess the sources and instream impacts of sediment inputs at the scale of individual stream reaches and small basins (e.g., Trimble, 1999). These rigorous studies continue to advance and verify sediment transport theory, but are typically too intensive and costly for application in regional or routine local assessments. Synoptic surveys used by management and regulatory agencies necessarily forsake intensive study at a few locations (reaches or watersheds) in favor of obtaining measurements from many locations across larger regions; they accomplish this by using streamlined protocols to describe channel morphology, bed particle size, and other features of stream physical habitat. A need exists for field and analytical approaches that allow synoptic habitat surveys to incorporate knowledge from more intensive research, so that these surveys can be used to test hypotheses concerning the effects of human activities on streambed particle size in a regional context.

Interpreting the extent of human influences on sediment in streams from regionally extensive surveys is difficult because, even in landscapes with uniform lithology and land use, bed particle size varies naturally in streams of different sizes and slopes. Therefore, it is essential to have some efficiently obtained measure of how much the bed surface particle size (e.g., D_{50} or percent fines) in a stream deviates from that expected based on natural controls in the absence of human activities. Among streams flowing within a region at the same slope, large, deep streams naturally tend to have coarser beds than small, shallow streams because the greater shear stresses of their deeper flows tend to quickly transport fine particles downstream (Lane, 1955; Leopold et al., 1964; Morisawa, 1968). The size composition of a streambed depends on the balance between the rates of supply of various sediment sizes to the stream and the rate at which the flow moves them downstream — i.e., the stream's sediment transport capacity relative to its sediment supply (Mackin, 1948; Schumm, 1971; Dietrich et al., 1989). The sediment supply rate and the type and size of particles delivered to a stream by upslope erosion and mass transport are influenced by basin characteristics, including lithology, topography, climate, vegetative cover, runoff characteristics, and land disturbances. On the other hand, the potential sediment transport competence and capacity of a stream are largely dependent on its slope, watershed area, and runoff regime, characteristics that determine the velocity and depth of water flow. Transport competence, the maximum size limit for particles that a stream can mobilize through bed shear stresses, can be lessened by bedforms, bank irregularities, large wood, and other channel features that increase hydraulic resistance and dissipate energy in turbulence (Buffington and Montgomery, 1999a). Transport capacity depends upon the amount of the bed surface exposed to competent shear stresses and the duration of competent flows.

By comparing the size range of streambed sediments with a stream's erosive competence (i.e., bed shear stress) during typical flood conditions, researchers have evaluated bed stability over a wide range of stream slopes, drainage areas, and bed particle sizes (e.g., Dingman, 1984; Dietrich et al., 1989; Gordon et al., 1992; Buffington, 1995; Montgomery et al., 1999). If the average size of particles making up a streambed surface is finer than the average size the stream is capable of moving, those sediments move frequently, rendering the bed relatively unstable. Such comparisons of observed bed particle size with critical diameter calculated from shear stress have been used to evaluate the effects of sediment supply (e.g., Buffington and Montgomery, 1999b; Montgomery et al., 1999), large-scale roughness elements such as large wood and bed forms (Buffington, 1995, 1998; Buffington and Montgomery, 1999a, 2001), or frequency of competent flows (e.g., Bledsoe et al., 2007). We calculate relative bed stability (RBS) here as the ratio of observed stream bed surface particle diameter divided by the critical, or mobile particle diameter (Dingman, 1984; Gordon et al., 1992). RBS is equivalent to the bed textural fining measure calculated by Buffington and Montgomery (1999a,b), and is also analogous to relative bed stability measures defined by Jowett (1989) as the ratio of critical bed particle entrainment velocity to actual near-bed velocity or by Olsen et al. (1997) as the ratio of critical shear stress to bankfull shear stress. In the sense that it is a comparison of bed particle size to the inferred maximum size that bankfull flows are competent to move, the RBS ratio is also conceptually similar to the bed stability ratio defined and discussed by Dietrich et al. (1989) as the median diameter of the stream bed armor layer divided by that of the substrate beneath that layer, which is taken to be the bedload. RBS is also analogous to the riffle stability index of Kappesser (2002), which estimates the mobile fraction of bed particles on a stream riffle by comparing the relative abundance of various particle sizes present on the riffle with the dominant large particles on an adjacent bar.

Although the potential reduction of sediment transport competence resulting from large scale bed form roughness and large wood is well known, detailed research approaches to quantify it are time-consuming, so have not been applied in broad regional surveys. We are not aware of any bed shear stress, critical diameter, or RBS formulations other than that of Kaufmann et al. (1999) that explicitly account for large-scale bedform roughness and large wood in a way that might be calculated from synoptic stream survey data. Their approach was developed to enable general evaluation of bed stability and anthropogenic sedimentation in regional ecological surveys. In this study, we modify the approach of Kaufmann et al. (1999) by using empirically derived relationships to compute an effective hydraulic radius (in effect partitioning shear stress), and by allowing the dimensionless critical shear stress (Shields parameter) in the critical diameter calculation to vary as a function of particle Reynolds number. The adjusted hydraulic

radius explicitly accounts for the reduction in bed shear stress available for sediment transport from the hydraulic resistance of large wood and longitudinal bedform roughness. We test our modified index (RBS*) by examining its association with natural and anthropogenic factors in to summer low flow probability sample of 104 wadeable stream reaches in the Coastal Ecoregion of Oregon and Washington, USA.

We suggest that hypotheses concerning sediment transport can be tested on regional scales using data from routine, relatively rapid physical habitat surveys, provided that specific measurement protocols are followed that adequately address a minimum set of key channel attributes required to estimate bankfull hydraulic resistance, bed shear stress, and particle size. The U.S. Environmental Protection Agency's (EPA) Environmental Monitoring and Assessment Program (EMAP) developed a well-defined field sampling protocol described by Kaufmann and Robison (1998) and later modified by Peck et al. (2006) that requires only ~3 h sampling time for a two-person field crew; we found it practical and adequate for obtaining the relevant measurements from wadeable streams. Data at individual streams are limited to relatively quick and simple measures made at low flow. Pertinent measurements include estimated bankfull channel dimensions, a longitudinal thalweg depth profile, water surface slope, a woody debris tally, and a systematic pebble count. These data are collected on relatively long reaches (40 wetted channel widths) and then summarized for each reach (see Kaufmann et al., 1999, and methods section for greater detail). We present and evaluate an approach that interprets these routine survey data in the context of sediment transport theory to estimate bed shear stress and assess the stability of streambeds under bankfull flow conditions. As a test of the potential utility of the RBS* index, we examine its association with human land use to evaluate expected relationships.

2. Objectives and hypotheses

Our primary objective is to derive an expression of RBS* that is adequate to accurately depict regional patterns in this stream characteristic and its association with likely geomorphic and anthropogenic controlling factors and influences. Furthermore, we want to restrict the intensity and sophistication of required field measurements to those that can be measured in routine, synoptic surveys over a wide range of natural conditions, including streams with large amounts of form roughness from features such as pools, channel constrictions, depth variability, and large wood. A reasonable test of RBS* would be a regional application in which this index responded as expected to influences on sediment supply and transport competence. We hypothesize that RBS* in relatively pristine streams will have values that are characteristic of their geoclimatic region or class of streams within that region, depending upon their natural lithology, soils, topography, climate, vegetation, and geomorphic setting (stream size, slope, constraint). We further hypothesize that RBS* will decrease in proportion to increases in sediment supply above that derived from the natural disturbance regime. To the extent that human land use intensity and extent have augmented sediment supply by increasing erosion rates above natural levels, RBS* should decline progressively across a gradient of increasing human disturbance.

3. Study area, field methods, and data reduction

The Pacific Northwest (PNW) coastal region is advantageous for applying our modified index of relative bed stability and testing its performance because of the wide range in stream gradients, channel form roughness, large wood loadings, natural land erosion potentials, and the levels and types of land disturbance in this region. Further, streambed sedimentation and bed stability have been identified as problems in the region (Nehlsen et al., 1991; Waters, 1995; Spence et al., 1996) and a synoptic probability survey of stream habitat and biota has been undertaken (Fig. 1; Herger and Hayslip, 2000). Models supporting the adjustment of bed shear stress to account for stream channel bedform roughness and wood loadings in the synoptic surveys were developed based on data from a separate study in 1984–1985 by Kaufmann (1987a) employing intensive dye-tracer experiments in streams of the Oregon Coast Range (Fig. 1). Those tracer experiments were conducted over a range of flow stages, channel complexity, and large wood loadings, including wood manipulations.

3.1. Synoptic surveys

For regional application and testing of RBS*, we analyzed data from one or more site visits to 104 stream reaches in the Coastal Range Ecoregion (Omernik, 1987) of Oregon ($n=57$) and Washington ($n=47$) that were surveyed in 1994–1996 by the Oregon Department of Environmental Quality and the Washington Department of Ecology in cooperation with the U.S. EPA (Herger and Hayslip, 2000). Hereafter, we refer to these surveys as the "PNW synoptic survey." These sites were selected as a probability sample using EMAP site selection protocols (Stevens and Olsen, 1999, 2004; Herlihy et al., 2000) and are representative of the population of first- through third-order (Strahler, 1957) streams delineated on 1:100,000-scale U.S. Geologic Survey topographic maps of the region (Fig. 1). In order to evaluate measurement and short-term temporal variability, 29 within-season revisits were made (normally by different field crews) to 19 sites over the time period 1994–1996, and all of the Oregon sites were revisited in the summer following a large storm in February 1996 (the 1996 data was only used in the variability study).

Field data collected in the regional surveys included measures of channel and riparian attributes, as well as observations of the type and extent of human disturbances. We summarize the relevant parts of the field protocol here; for more detail, consult Kaufmann and Robison (1998). Procedures for calculating stream reach summaries of channel and riparian characteristics from these detailed data are described by Kaufmann et al. (1999). Sample reach lengths were ~40 times their summer season wetted width, but no less than 150 m. The field data were collected from longitudinal profiles and from 11 equally spaced cross sections with associated streamside riparian plots on each side (visually estimated 10 m × 10 m).

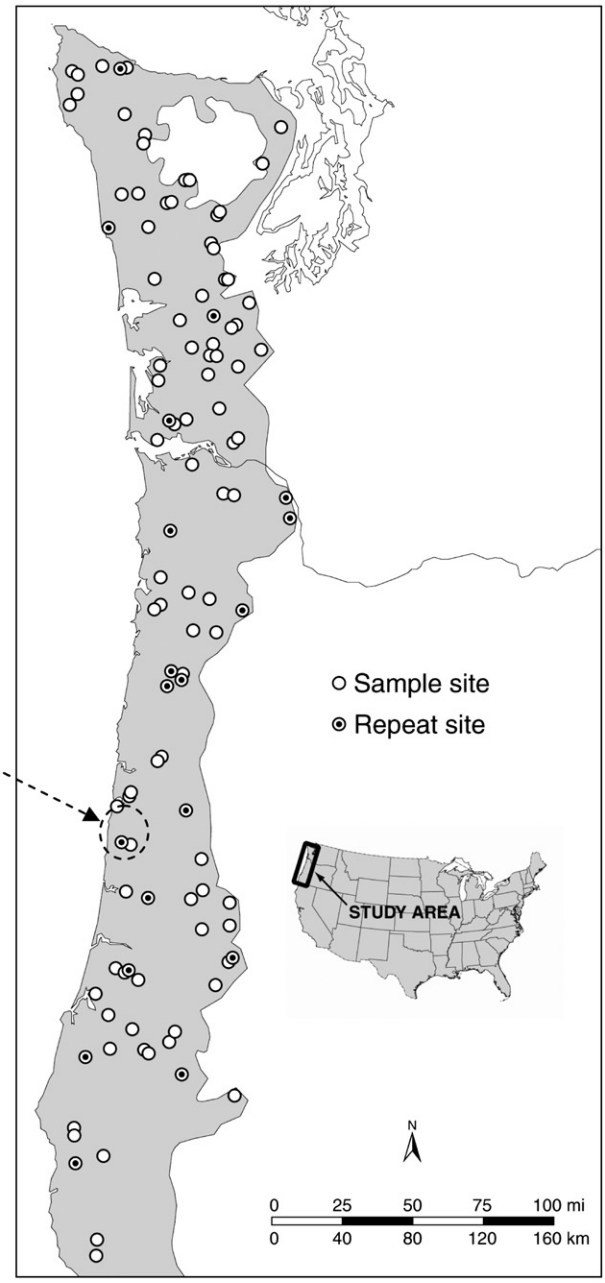

Fig. 1. Map of Coastal Oregon and Washington, showing stream reach sites in 1994–1996 synoptic survey by Oregon Department of Environmental Quality, Washington Department of Ecology, and the USEPA. Dashed arrow and circle show location of intensive dye tracer and wood manipulation studies in the Cummins Creek Wilderness Area reported by Kaufmann (1987a,b).

Channel measurements on each sample reach included a longitudinal survey of maximum (thalweg) depth at 100 equally spaced points (150 on streams <2.5 m wide) and other measurements made at 11 cross sections equally spaced at every 10th thalweg measurement location (every 15th on streams <2.5 m wide). The measurements taken at the cross sections included wetted and bankfull width, bankfull height above the low flow water surface (using a stadia rod and hand-held level), visual particle size determinations and depth measurements at 5 equally spaced points across the wetted channel, and water surface slope between adjacent cross sections (using stadia rod and hand-held clinometer). Reach means and standard deviations of thalweg depth, bankfull dimensions, wetted width, and other morphologic descriptors were calculated from these measurements. Combined with mean reach slope, long profiles of thalweg depth were used to calculate mean residual depth according to procedures described by Robison and Kaufmann (1994). Mean residual depth is a flow-independent index of reach-scale pool volume and large-scale roughness (see Bathurst, 1981; Kaufmann, 1987a; Keim and Skaugset, 2002; Keim et al., 2002), a reach-scale interpretation of the residual pool concept, where individual residual pools are defined as those portions of a stream that would contain water at zero discharge because of the damming effect of their downstream riffle crests (Lisle, 1982; Mossop and Bradford, 2006). Bankfull height was estimated in the field from channel, bank and floodplain geometry, deposition features with fine sediments, riparian vegetation, and flood height evidence. Bankfull thalweg depth was then calculated as the sum of the reach mean bankfull height above water level plus mean thalweg depth, both measured at the summer low flow (see Kaufmann et al., 1999).

Large wood pieces ($\geq$10 cm in diameter and $\geq$1.5 m long) within the bankfull channel were tallied by size class along sample reaches (three length and four diameter classes), and data were summarized as estimated wood volume per m^2 of bankfull channel area. Vegetation cover and type were visually estimated for each of three vegetation layers (ground cover, mid layer, and canopy) within each of the 11 pairs of streamside riparian plots. Mean areal cover values for these riparian vegetation layers were calculated as reach-scale summaries. At and beyond each riparian plot, the presence and proximity of 11 categories of streamside human influences were recorded (row crops, pasture, dams and revetments, buildings, pavement, roadways, pipes, landfill or trash, parks/lawns, logging operations, and mining activities). A proximity-weighted disturbance index (W1_HALL) was calculated by tallying the number of left and right bank riparian stations at which a particular type of disturbance was observed, weighting each observation according to its proximity to the stream and then averaging over all 11 transects on the reach (Kaufmann et al., 1999). Scores of the disturbance index ranged from 0 to 5 in this data set, reflecting a range from low to high riparian disturbance.

Stream reach water surface slope (%) was calculated as the arithmetic mean of 10 water surface gradient measurements from hand held clinometer sightings on survey rods between sequential pairs of the 11 equally spaced transects. Particle size of the wetted streambed surface was quantified by means of a systematic pebble count, in which 55 particles (5 from each of 11 channel cross sections) were selected and visually classified according to size categories. Whole-reach bed surface particle size summaries included the geometric mean diameter (D_{gm}) and the percentages of bedrock (>4000 mm diameter), boulders (250–4000 mm), cobbles (64–250 mm), coarse gravel (16–64 mm), fine gravel (2–16 mm), sand (0.06–2 mm), fines (<0.06 mm), and organic detritus. D_{gm} was calculated by nominally assigning to each particle the geometric mean diameter of the upper and lower bounds of its size class (e.g., 5.66 mm for fine gravel) and then calculating the geometric

mean as the antilog of the arithmetic mean of the logarithms of those frequency-weighted class midpoint values. Bedrock and fines, respectively, were assigned class midpoint values of 5660 mm and 0.0077 mm.

We used a composite riparian condition index (RCOND) defined by Kaufmann and Hughes (2006) from field data tallying evidence of streamside human activities and the cover and structure of riparian vegetation. The index decreases with streamside human activities (W1_HALL) and increases with large diameter tree cover (XCL) and riparian vegetation complexity (XCMGW, the sum of areal cover of woody vegetation in the tree, shrub, and ground cover layers). The riparian habitat measures contributing to RCOND are described in detail by Kaufmann et al. (1999). The index RCOND was defined as follows:

$$\mathrm{RCOND} = \{(\mathrm{XCL})(\mathrm{XCMGW})[1/(1+\mathrm{W1\_HALL})]\}^{1/3} \quad (1)$$

We based our estimate of the level of human activity and disturbance within the contributing drainages of our sample sites on road densities (Rd_Denkm) calculated from digital road coverages (TIGER, 1990, http://www.census.gov/geo/www/tiger). We further defined ordinal watershed disturbance classes (W_CLS) according to Hughes et al. (2004) as Low: Rd_Denkm < 1.3 km/km^2; Medium: Rd_Denkm ≥ 1.3 to ≤ 1.9; and High: Rd_Denkm > 1.9.

We used an index of watershed + riparian condition combining the continuous riparian condition index with road density as defined by Kaufmann and Hughes (2006):

$$\mathrm{WRCOND} = \{[1/(1+(\mathrm{Rd\_Denkm}/6))]\mathrm{RCOND}\}^{0.5} \quad (2)$$

In addition, we combined riparian and watershed condition class as described by Hughes et al. (2004) to define DISTLEVEL, an ordinal watershed + riparian anthropogenic disturbance variable. We modified the Hughes et al. (2004) disturbance classes by collapsing the two highest and the two lowest classes to yield five DISTLEVEL classes ranging from 1 = lowest disturbance to 5 = highest disturbance.

We partitioned the total variance into between- and within-site components (see Kaufmann et al., 1999; Larsen et al., 2004), interpreting the square root of the within-site variance ($\mathrm{RMS_{rep}}$) as a measure of the precision or replicability of field measurements. $\mathrm{RMS_{rep}}$ is equivalent to the root mean square error (RMSE) relative to the site means (e.g., as applied by Kaufmann et al., 1999), that is, the pooled repeat visit standard deviation of each repeated measurement relative to its site mean.

3.2. Hydraulic resistance studies

Data to examine the relationship between hydraulic resistance and form roughness used in the adjustment of RBS* for wood and form roughness were collected by Kaufmann (1987a) in a series of 41 dye-transit experiments on 16 wadeable stream reaches in western Oregon (Fig. 1). The climate, vegetation and geology of these basins are similar to other parts of the PNW coastal ecoregion. For the purposes of quantifying the relationship between hydraulic resistance and channel roughness, however, it was more important that these stream reaches included a very wide range of large wood and residual pool volume. Dye transit and channel morphology were examined on fourteen 100 m (~25–30 × wetted width) study reaches in the Cummins Creek Wilderness Area along the central Oregon coast, and in two other study reaches outside the Wilderness between June 1984 and August 1985. A full suite of measurements (Table 1) were taken on each stream reach, with three to five repetitions of selected measurements on each reach over a range of flow conditions, including measurements on some reaches during large storms. The study included before and after measurements on four reaches (and three untreated control reaches) where the U.S. Forest Service had placed varying amounts of large logs in the stream channel. Sample reach data included discharges from 0.02 to 0.62 m^3/s, reach-scale mean advective velocities from 0.065 to 0.29 m/s, channel gradients from 2.6 to 8.3%, coefficient of variation in thalweg depth (SDd_{th}/d_{th}) from 0.19 to 0.75, wood volumes from 0.99 to 105 m^3/100 m, and reach-scale Manning's roughness coefficients (n_t) from 0.10 to 0.76 (Table 1).

The methods used for measuring hydraulic resistance and channel morphology during the dye transit experiments at the 16 intensely studied stream reaches are described in detail by Kaufmann (1987a). Detailed longitudinal profiles of bottom elevation, depth, wetted width, water velocity, pool volume, and the number and dimensions of large wood pieces were obtained on each reach. Hydraulic time of travel and dispersion characteristics of instantaneous slug releases of a known mass of dye tracer in study reaches were determined using both

Table 1
Sample distributions of selected channel and hydraulic characteristics of 16 intensive study reaches in the Oregon Coast Range reported by Kaufmann (1987a)

Variable	Median	Range
Q_{meas} = discharge at sample time (m^{3}s^{-1}) from dye transit	0.042	0.019–0.62
U_c = reach-scale mean advective velocity (m.s^{-1}) from dye transit	0.17	0.065–0.29
S_s = mean slope of reach water surface (%)	3.4	2.6–8.3
W = mean wetted width (m)	3.1	2.3–5.2
A_{xs} = effective mean flow cross section (m^2) = Q_{meas}/U_c	0.26	0.15–2.67
d_h = effective mean hydraulic depth (m) = $A_{xs}/W \simeq R$	0.082	0.060–0.29
SD$W/W$ = (Standard deviation wetted width)/(mean wetted width)	0.30	0.15–0.42
d_{th} = mean depth at thalweg (m)	0.18	0.12–0.50
SDd_{th} = Standard deviation of thalweg depth (m)	0.058	0.027–0.22
SDd_{th}/d_{th} = coefficient of variation in thalweg depth	0.37	0.19–0.75
d_{res} = mean residual depth at thalweg (m)	0.033	0.012–0.11
d_{res}/d_{th} = mean residual depth proportion	0.19	0.088–0.49
Large wood in bankfull channel (number of pieces/100 m)	28	6–97
Large wood volume in bankfull channel (m^3/100 m)	7.7	0.99–105
Large wood mean piece volume (m^3)	0.33	0.11–2.5
Wd/d_h = wood relative depth = (wood volume/channel area)/ d_h	0.11	0.015–0.95
Total hydraulic resistance (dye transit), C_t (note $C_t = f_t/8$)	1.0	0.25–11
Total hydraulic resistance (dye transit), f_t	8.2	2.0–87
Total hydraulic resistance, n_t (with SI units $n_t = R^{1/6}C_t^{1/2}/g^{1/2}$)	0.22	0.10–0.76

continuous and discrete sampling methods. The time-of-travel of the center of mass of the dye concentration versus time curve was used to calculate a mean water velocity, as recommended by Calkins and Dunne (1970). This was interpreted to be the mean advective velocity of the water mass in the stream channel during each experiment. Discharge at the time of sampling was also calculated from the dye concentration-time curves using methods described by Hubbard et al. (1982). Darcy–Weisbach friction factor estimates for each reach dye experiment were calculated from discharge, advective mean velocity, and channel morphology according to the following formulation, employing flow continuity considerations and a wide channel approximation:

$$f_t = (8gRS_e)/U^2 \simeq \{8g(Q/UW)S_s\}/U^2 = (8gQS_s)/WU^3 \quad (3)$$

where:

f_t = reach-scale Darcy–Weisbach hydraulic resistance "friction" factor;
g = gravitational acceleration;
R = mean hydraulic radius;
S_e = mean energy gradient between two ends of reach;
S_s = mean water surface slope between two ends of reach;
Q = volumetric discharge rate, from time-concentration plot of known dye mass;
U = mean advective velocity in reach; and
W = mean wetted width.

4. Theoretical basis for relative bed stability index

In evaluations of the stability of whole streambeds (vs. individual bed particles), observed bed surface particle size is typically represented as the median (D_{50}) or the geometric mean (D_{gm}) diameter determined from a stream bed pebble count (e.g., Wolman, 1954). For calculating critical bed particle diameter in a natural stream, it is necessary to estimate average streambed tractive force, or shear stress, for some common reference flow condition likely to mobilize the streambed. Bankfull discharge is a commonly used and logical choice for this purpose, as it has been shown to approximate the effective discharge (i.e., the discharge responsible for the majority of sediment transport) in many cases (e.g., Wolman and Miller, 1960; Emmett and Wolman, 2001), although substantial bedload transport can occur at discharges below bankfull conditions in "live-bed" streams typified by naturally sand-bedded channels (Howard, 1980) and in some gravel-bed channels (Wilcock, 1997, 1998; Bledsoe and Watson, 2001). Mueller et al. (2005) reported that significant bedload transport was initiated at an average of 67% of bankfull discharge in 45 gravel-bed streams they studied and speculated that "…bank-full channel geometry of gravel- and cobble-bedded streams is adjusted to a relatively constant excess shear stress [above that required to initiate bedload transport]… across a wide range of slopes." Furthermore, bankfull channel dimensions generally reflect the dominant flows for channel maintenance through bedload transport (regardless of recurrence interval) and can generally be estimated in the field during low flow conditions. For these reasons, we selected bankfull flow as our reference flow condition.

The average shear stress acting on the stream bed at bankfull flow can be expressed as:

$$\tau_{bf} = \rho g R_{bf} S \quad (4)$$

where τ_{bf}=bankfull channel bed shear stress [N m^{-2}], ρ=mass density of water [kg m^{-3}], g=gravitational acceleration [m s^{-2}], R_{bf}=bankfull channel hydraulic radius [m], and S=energy slope, approximated by channel water surface slope [m/m]. This estimate of τ_{bf} pertains to flow conditions that are temporally steady and spatially uniform at the scale of the stream reach. These conditions for steady and quasi-uniform flow were approximated in our sample streams (by the criteria of Paola and Mohrig, 1996), as a result of making measurements over long reaches under conditions during which discharge was nearly constant and using reach-average values in the calculations. Reach-scale estimates may be less accurate and precise than spatially explicit reach characterizations of τ_{bf}, but can give acceptable first-order approximations for evaluating reach-scale classifications of bed stability (Lisle et al., 2000).

Bed particle movement by erosion is dependent upon particle size, water depth and velocity, the difference between the mass densities of particles and fluid, and the shape and arrangement of particles (e.g., packing, armoring, gradation, and embeddedness). The shear stress necessary to move a particle, critical shear stress (τ_c), was first estimated by Shields (1936) as a function of particle diameter as

$$\tau_c = \theta(\rho_{sed} - \rho)gD \quad (5)$$

where θ=dimensionless critical shear stress for incipient motion (Shields parameter); $\rho_{sed}-\rho$=the difference between the mass densities of sediment particles and water [kg m^{-3}]; and D=the bed surface particle diameter [in m, if τ_c is in Newtons per m^2].

By setting $\tau_c=\tau_{bf}$ and solving for D, we calculate the *critical* (or maximum) diameter of particles that can be transported at bankfull flow (D_{cbf}). Because it is calculated from a representation of the *average* bankfull shear stress within a long reach, D_{cbf} is an estimate of the average (e.g., geometric mean or median) bed surface particle critical diameter within the reach:

$$D_{cbf} = (\rho g R_{bf} S)/[\theta(\rho_{sed} - \rho)g] \quad (6a)$$

Substituting g=9.81 m s^{-2}, ρ_{sed}=2650 kg m^{-3} (average density for silicate minerals), and ρ=998 kg m^{-3} for freshwater at 20 °C, Eq. (6a) simplifies to the following expression, where D_{cbf} and R_{bf} are in the same units:

$$D_{cbf} = 0.604 R_{bf} S/\theta \quad (6b)$$

Finally, we calculate RBS (the measure of relative bed stability) as the ratio (D_{gm}/D_{cbf}) of the observed bed surface particle geometric mean diameter divided by the average critical diameter at bankfull flow:

$$\mathrm{RBS} = D_{gm}/D_{cbf} = D_{gm}/(0.604 R_{bf} S/\theta) = 1.66\theta D_{gm}/(R_{bf} S) \quad (7)$$

Note that setting $\theta = 0.044$ (per Yalin and Karahan, 1979, for mixed gravel-bed streams) yields Dingman's (1984) expression for critical diameter in mixed gravel-bed streams, $D_{cbf} = 13.7 R_{bf} S$, used by Kaufmann et al. (1999) in their expression $RBS^* = D_{gm}/(13.7 R_{bf}{}^* S)$.

5. Adapting theory to regional surveys of complex, natural streams

Regional assessments of sedimentation have been seriously limited by lack of practical means of sampling and then interpreting data from stream surveys. The expression for RBS in Eq. (7) is strictly applicable to uniform flow in relatively simple channels that lack large-scale roughness elements or changes in cross section that reduce the reach average shear stress exerted on bed particles. For proper use in most natural streams Eq. (7) must be adjusted to account for channel roughness and consequent reductions in both bed shear stress and competent D_{gm} (Buffington and Montgomery, 1999a,b). For our application, therefore, we must calculate a new index (RBS*) that explicitly accommodates the influence of these features of natural channels by modifying the denominator (D_{cbf}) to adjust for channel complexities typical of natural streams, such as large wood and longitudinal variation in stream depths and flow cross-sectional area.

5.1. Bankfull hydraulic radius estimate

Our approach for estimating τ_{bf} from stream survey data requires a reasonable approximation of the mean hydraulic radius at bankfull flows, if possible based on the mean thalweg depth to reduce data requirements. Robison and Beschta (1989) examined longitudinal thalweg depth profiles and variation in cross-sectional depth of wadeable stream channels during low flow stage in a wide range of stream sizes and geographic locations in western North America. They showed a triangular cross section ($d_h = 0.5 d_{th}$) to be a reasonable approximation for summer (low) flows, where d_h = mean depth of cross sections, and d_{th} = mean depth of thalweg longitudinal profiles. In comparison, Faustini (unpublished data) examined similar data from EMAP surveys of 1328 wadeable streams across the Western U.S. (Stoddard et al., 2005a,b) and obtained an average relationship for mean depth of estimated bankfull cross sections that corresponds with a roughly parabolic or trapezoidal channel shape, $d_{h-bf} = 0.65 d_{th-bf}$, where the additional bf subscript denotes bankfull conditions ($R^2 = 0.92$; RMSE = 0.106 m; $p < 0.0001$). For our calculations, we assumed $W >> d_h$ and estimated $R_{bf} \simeq d_{h-bf} = 0.65 d_{th-bf}$.

5.2. Shear stress adjustments for large-scale roughness

The *effective* shear stress exerted on particles making up the bed of a natural stream channel is typically less than the *total* shear stress value (τ_{bf}) calculated with the unadjusted R_{bf} value because of energy losses from roughness characteristics including pools, bank irregularities, bars, and large wood (Einstein and Barbarossa, 1952; Nelson and Smith, 1989; Buffington, 1998). One approach to partitioning shear stress into its components is to partition the hydraulic radius in the shear stress expression into parts that exert force on the bed particles, wood, and other roughness elements (e.g., Einstein and Barbarossa, 1952; Engelund, 1966).

Kaufmann et al. (1999) partitioned R_{bf} directly by subtracting the approximate roughness heights of large wood and pool-riffle scale channel bed irregularities. They calculated the effective hydraulic radius, $R^*_{bf(1999)} = (R_{bf} - R_{wood} - R_{pool})$, by subtracting from R_{bf} the large wood "mean depth" (R_{wood} = m^3 wood volume per m^2 channel surface area = m wood "depth"), and the cross section mean residual depth (R_{pool} = one-half the thalweg mean residual depth, approximating mean residual depth in a triangular cross section). That approach assumes that the mean roughness "heights" of large wood and pool-riffle structure translate directly to reductions in effective hydraulic radius. Other approaches for directly partitioning R_{bf} require more intensive data than typically collected in synoptic stream surveys to describe the size, shape, spacing, and orientation of roughness elements in relation to stream flow (e.g., Shields and Gippel, 1995; Buffington, 1998; Buffington and Montgomery, 1999a; Wilcox et al., 2006).

We adjusted R_{bf} differently than did Kaufmann et al. (1999), basing our adjustment on the assumption that hydraulic resistance is additive (e.g., Cowan, 1956; Chow, 1959) and can be partitioned more directly than water depth or roughness heights. That is, one can express total hydraulic resistance as the sum of separate resistance components, $C_t = C_p + C_w + C_f + \ldots C_i$, where $C_t = gRS/U^2 = f/8 = gn^2/R^{1/3}$, a dimensionless coefficient of hydraulic resistance (denoted k_t by Dingman, 1984), where U = mean advective water velocity, f = Darcy–Weisbach friction factor, n = Manning's n (all quantities are in SI units), and subscripts t, p, w, f, and i (respectively) denote total hydraulic resistance and its subcomponent resistances derived from bed particles, wood, large-scale channel form roughness, and other sources of resistance. (C_t should not be confused with the dimensionless form of the Chezy resistance coefficient, Cz, which is an inverse measure of hydraulic resistance related to C_t as follows $Cz = U/g(RS)^{0.5} = C_t^{-0.5}$.) We simplified the partitioning of total hydraulic resistance to define the proportion from particle ("grain") resistance, C_p/C_t, and then used a function of this ratio to estimate the proportion of the flow depth attributable to the resistance from bed particles. (Note that this is not equivalent to the flow depth that would result if roughness other than particles were physically removed from the channel). An advantage of this approach is that we do not have to directly estimate the separate resistances resulting from other sources such as form roughness (e.g., pools) and wood (e.g., see discussion by Wilcox et al., 2006, concerning problems in overestimating unknown resistance components by subtraction of measured components from total resistance).

From the expression for total shear stress as a function of mean velocity (U) and total hydraulic resistance C_t,

$$\tau_t = \rho g R S = \rho U^2 C_t \tag{8}$$

(Dingman, 1984), and the Chezy expression (Eq. (9a) below) modified from Dingman (1984) for discharge in a uniform flow cross section (A_{xs}), we derive the expected approximate increase

in R_{bf} that would accompany an incremental increase in hydraulic resistance, C_t, under conditions of constant discharge. In order to examine unit discharge, we assume $W>>R$ (i.e., wide channel) and minimal increase in width as a result of roughness-caused depth increases (d_h=mean depth$\simeq R$, and W_p=wetted perimeter$\simeq W$ when $W>>d_h$). From the Chezy equation,

$$Q = (1/C_t)^{1/2} A_{xs} (gRS)^{1/2} \tag{9a}$$

Dividing both sides of Eq. (9a) by A_{xs}, squaring, and making use of the assumptions stated above,

$$(Q/A_{xs})^2 = (1/C_t)gRS = (1/C_t)g\left[(d_h W)/W_p\right]S \simeq (1/C_t)g[(d_h W)/W]S \tag{9b}$$

$$Q^2/\left(W^2 d_h^2\right) \simeq (1/C_t)g d_h S \tag{9c}$$

$$Q^2/W^2 \simeq (1/C_t)g d_h^3 S \simeq (1/C_t)gR^3 S \tag{9d}$$

If we set Q, W, and S constant in Eq. (9d), but allow C_t to vary, then R is proportional to $C_t^{1/3}$, suggesting that flow depth attributable to a particular subcomponent of hydraulic resistance is related to the ratio of that subcomponent to the total hydraulic resistances as follows for particle-derived resistance:

$$R_p/R_{bf} = \left(C_p/C_t\right)^{1/3} \tag{10a}$$

hence:

$$R_p = R_{bf}\left(C_p/C_t\right)^{1/3} \tag{10b}$$

Because $\tau_{bf}=\rho g R_{bf} S$, the hydraulic resistance ratio C_p/C_t allows us to estimate τ_p by adjusting R_{bf} as follows:

$$\tau_p = \rho g R_{bf}\left(C_p/C_t\right)^{1/3} S \tag{11}$$

5.3. Estimating components of the hydraulic resistance ratio for shear stress adjustment

To apply Eq. (11), we must estimate C_p, hydraulic resistance resulting from bed particles, and C_t, the total hydraulic resistance in the channel. It is advantageous to base these estimates on relative submergence of particles or bed forms, if possible, so that resistance can be calculated at any flow depth.

5.3.1. Hydraulic resistance resulting from bed particles

We use a form of the Keulegan equation to estimate particle resistance C_p as a function of the relative submergence of bed particles (Keulegan, 1938). We based the relative submergence of bed particles on the observed mean depth, rather than either the adjusted depth (R_p) or the estimated depth that would result if bedforms were absent, because we are estimating the component resistance of particles in the presence of other sources of roughness. (Note that the greater submergence of particles leads to a smaller estimate of C_p than would be the case for the same discharge and slope in the absence of other sources of roughness.) Millar and Quick (1994) and Millar (1999) recommended setting the roughness height k_s equal to D_{50} rather than to larger best fit values (multiples of D_{50} or D_{84}) reported by others (see Table 1 in Millar, 1999). These researchers chose this approach to avoid incorporating the effects of form roughness into the resistance estimate. We employed this formulation, substituting D_{gm} for D_{50}:

$$C_p = f_p/8 = (1/8)\left[2.03 \quad \text{Log} \quad \left(12.2 d_h/D_{gm}\right)\right]^{-2} \tag{12}$$

where d_h/D_{gm}=particle relative submergence; and all quantities are in SI units. We set a minimum value of C_p=0.002 (Mannings $n\simeq 0.01$). This is equal to the value calculated for relative submergence of 1.0-mm diameter sand at the median bankfull depth (0.71 m) for streams in our regional data set, similar to that for very smooth artificial channels, and approximately one-half of the equivalent Mannings n value of 0.020 shown by Chow (1959, Table 5-5) for a smooth natural channel with fine bed particles and minimum channel complexity, obstructions, and vegetation.

5.3.2. Total hydraulic resistance

Prediction of total hydraulic resistance (C_t) using existing empirical or theoretical approaches is notably difficult in natural streams, which commonly have complex channel morphology with substantial roughness in addition to that from bed particles alone. In an examination of boundary shear stress, Wiberg and Smith (1991) noted that, although velocity profiles are markedly non-logarithmic in coarse gravel-bedded streams with high relative roughness (e.g., $D_{84}/d_h\simeq 0.1$ to 0.5), nearly log-linear relationships between measured mean velocity and relative roughness (D_{84}/d_h) have been observed in natural streams. Presumably, this is why equations derived assuming logarithmic velocity profiles (e.g., those of Hey, 1979 and Leopold, 1994) are generally good predictors of the Darcy–Weisbach friction factor (f_t) in channels of relatively simple morphology. Bathurst (1981) observed, however, that such equations can greatly underestimate resistance in complex channels (e.g., those with large bedforms), presumably because they do not account for all scales of roughness present. He further suggested that estimates of resistance in more complex channels could be improved by incorporating bar resistance, which he took to be total resistance minus particle resistance (neglecting other sources of resistance such as wood, meander beds, and vegetation), and which he argued could probably be calculated directly from residual depth. See also Lisle (1982) for a definition and discussion of residual pool depth; and Kaufmann (1987a) and Kaufmann et al. (1999) for application of the concept to the reach scale and for a computational definition of mean residual depth.

5.3.3. Influence of form roughness

Recognizing that logarithmic velocity profiles cannot be assumed in channels containing very large roughness elements, some recent approaches have departed from this assumption by modeling flow using a mixing layer analogy. These approaches model hydraulic resistance as the result of momentum dissipation occurring when rapidly moving water mixes into a

very slow or nonmoving zone within the shelter of the roughness elements (Wiberg and Smith, 1991; Katul et al., 2002; Wu et al., 2005), roughly analogous to the two-compartment transient storage "dead zone" model proposed by Sabol and Nordin (1978) to explain advection and dispersion of solutes in dye transit studies.

Based on dye transport and surveys of channel morphology in wadeable Oregon Coast Range streams, Kaufmann (1987a) reported that, while grain (particle) resistance calculated using the equation of Bathurst et al. (1979) accounted for 29 to 40% of resistance (f_t) in relatively simple channels at low to moderate flows, it accounted for as little as 2 to 7% of f_t in complex channels with abundant wood in addition to flow expansions and contractions associated with pools and spill resistance due to steps and plunges. Similarly, spill resistance, calculated by subtraction, amounted to 80–90% of the flow resistance measured by Curran and Wohl (2003) during low flows in natural step pool channels with large woody debris and by Wilcox et al. (2006) in flume experiments simulating these conditions. MacFarlane and Wohl (2003), studying step-pool channels with no large woody debris, also found total hydraulic resistance to be dominated by sources other than bed particles. Neither Wilcox et al. (2006) nor MacFarlane and Wohl (2003) reported satisfactory models to predict total resistance or spill resistance from channel morphology measured in their studies. Curran and Wohl (2003), however, reported that 43% of the variation in f_t could be explained by the coefficient of variation in hydraulic radius measurements over their study reaches, but did not report a prediction equation.

Kaufmann (1987a), however, showed that hydraulic resistance was inversely related to the relative submergence of bedforms and other large-scale roughness elements (riffles, pools, steps), and these could be quantified by the ratio of mean thalweg depth (d_{th}) to mean thalweg residual depth (d_{res}). He interpreted d_{th}/d_{res} as an expression of relative submergence of bedforms (e.g., riffles and pools), analogous in concept to Wohl and Merritt's (2005) definition of "relative form roughness," the ratio of hydraulic radius to bedform height (which is actually a relative submergence index). The inverse hydraulic resistance measure, $(8/f_t)^{0.5} = U/U* = (U^2/gRS)^{0.5}$, back-calculated from mean advective dye transport velocity, was log-linearly related to relative submergence of residual depth [$(8/f)^{0.5} = 0.62\ Ln(d_{th}/d_{res})$, $R^2 = 0.57$, $n = 40$]. The standard deviation of thalweg depth (SDd_{th}) has been interpreted as an indicator of the variability of bed topography (Kaufmann, 1987a; Madej, 2001). Kaufmann (1987a) further observed that the close relationship between mean residual depth, d_{res}, and the standard deviation of thalweg depth, SDd_{th} ($R^2 = 0.90$), also allowed an alternative estimation of hydraulic resistance using d_{th} and SDd_{th} to represent bedform relative submergence. He reported that the (inverse) hydraulic resistance measure was nearly log-linearly related to the (inverse) coefficient of variation in thalweg depth [$(8/f)^{0.5} = Ln(d_{th}/\mathrm{SD}d_{th})^{0.92}$, $R^2 = 0.60$, $n = 40$]. Hydraulic resistance was quantified from the velocity of the centroid of the dye tracer concentration-time curves in Kaufmann's Oregon Coast Range stream studies, in which discharge and water surface slope ranged from 0.019 to 0.62 $m^3 s^{-1}$ and 2.6 to 8.3%, respectively; f_t ranged from 2.0 to 87, d_{res}/d_{th} from 0.088 to 0.49, and SDd_{th}/d_{th} from 0.19 to 0.75 (Table 1).

Except in relatively simple stream channels, the values of f_t measured by Kaufmann (1987a) were considerably higher at any given relative submergence than those predicted by the equations of Hey (1979), Bathurst et al. (1979), or Leopold (1994), which are based on relative submergence of particles. Curran and Wohl (2003) also reported that the flow resistances they measured in step-pool streams in Washington State substantially exceeded those estimated using Jarret's (1984) equation for Manning's n or Mussetter's (1989) equation for Darcy–Weisbach f. These results suggest that the hydraulic resistance from bedforms and wood clearly dominated that from particles in the streams studied, and that neither Keulegan formulations nor published empirical formulations relating hydraulic resistance to slope, basin area, etc., were adequate for small streams with complex morphology. Kaufmann's (1987a) research also supports the suggestion of Bathurst (1981) that the portion of roughness from pools and other vertical variations in channel cross-sectional area (bar resistance) might be represented by the mean residual depth, which is essentially a measure of the average height of longitudinal bedform roughness elements such as riffle crests. Further, those results suggest that, at least during low to moderate flows, bedform relative submergence (*sensu* Kaufmann, 1987a; Wohl and Merritt, 2005), represented by the ratio of d_{th} to d_{res} or SDd_{th}, might be treated much like particle relative submergence in the empirical prediction of hydraulic resistance from these roughness features.

5.3.4. Influence of large wood

Particularly in small streams draining forested areas, large in-channel wood (large woody debris or LWD) can be a major component of hydraulic resistance that is related to and interacts with pools and variations in depth and width (Buffington and Montgomery, 1999a). Manga and Kirchner (2000) showed that woody debris covering <2% of the streambed can contribute about half of the total hydraulic resistance in a stream reach. They also showed that wood additions increased total shear stress, but reduced that borne by particles at the bed surface. Based on Petryk and Bosmajian's (1975) model of energy loss per channel length from large LWD as the result of drag on a series of solid obstructions, Shields and Smith (1992) estimated the friction factor from large woody debris (f_w) as the product of four times the flow depth, a drag coefficient for LWD (assumed to be 1.0; Petryk and Bosmajian, 1975), and the roughness concentration of LWD. They cited Li and Shen (1973) in defining the average roughness concentration per unit length of the channel as the sum of the cross-sectional areas of LWD pieces and formations in the plane normal to flow divided by the product of width, depth, and channel length. This depiction of roughness concentration is similar to viewing LWD as a relative roughness height in the channel cross section profile. Wilcox et al. (2006) reported that combinations of LWD and step pools dominated the total resistance in flume studies, mostly by an interaction with bedforms and bed particles as described by Curran and Wohl (2003).

Shields and Smith (1992) measured friction factors in treatment and control reaches of a sand-bed river before and after LWD removal. Friction factors were 400% greater in uncleared reaches at base flow but declined to a level about 35% greater than that for cleared reaches at higher flows. Predicted friction factors were within 35% of those measured at higher flows. Kaufmann (1987a) described results in essential agreement with those obtained by Shields and Smith (1992) in similar experiments in which LWD was added to gravel-bedded streams in coastal Oregon. He showed that both large wood additions (7 to 57 m^3/100 m placed in four reaches) and among-stream differences in wood volume (from 0.99 to 105 m^3/100 m) were closely associated with hydraulic resistance, morphometric measures of roughness, and transient hydraulic storage "dead zone" volume proportion back-calculated from curves of dye concentration versus time using the model of Sabol and Nordin (1978). In Kaufmann's experiments, LWD effects on friction factor and morphometric measures of channel roughness increased over time elapsed since the wood was placed in the channels, and this was observed to be caused by the interaction of LWD with streamflows in scouring the bed. Effects were minor immediately after wood placement and before any opportunity for bed scouring. However, one year later, after higher flows, post/pre-treatment proportional additions of LWD were strongly correlated with and post/pre-treatment values of both SDd_{th} ($R^2=0.88$) and d_{res} ($R^2=0.91$). For example, a ten-fold increase in wood volume resulted in a 35% increase in SDd_{th} and an 84% increase in d_{res} in the treated reaches. As observed by Shields and Smith (1992), Kaufmann (1987a) reported declines in hydraulic resistance from added wood with increases in flow stage that were proportional to increases in the relative submergence of these roughness elements.

5.3.5. Modeling the combined effect of bedform roughness and wood on hydraulic resistance

Recognizing the interaction of wood and pool resistances and the difficulty of separately determining these components and unambiguously relating their sum to total resistance, we opted to develop a relationship to estimate total hydraulic

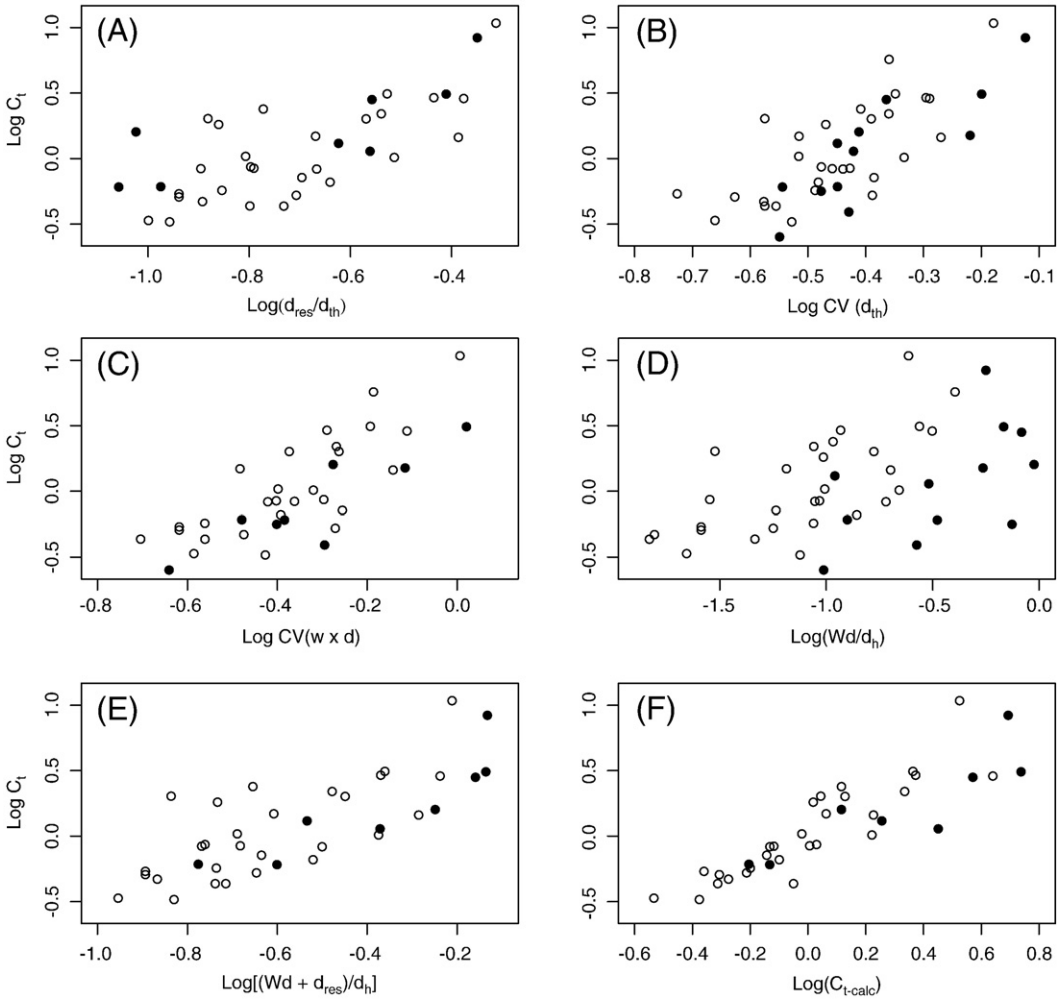

Fig. 2. Reach-scale total hydraulic resistance, Log(C_t) measured by dye tracer experiments versus morphologic channel roughness measures: (A) relative residual depth, Log(d_{res}/d_{th}); (B) relative depth variation, Log(SDd_{th}/d_{th}); (C) relative width-depth product variation, Log(SD$w\times d_{th}$)/($w\times d_{th}$); (D) wood volume proportion, Log(Wd/d_h)=(m^3 wood/m^2 bankfull channel area)/mean water depth; (E) residual pool+wood relative roughness, Log[($Wd+d_{res}$)/d_h]; (F) predicted Log(C_t) from regression Eq. (13a). Solid circles are reaches in which large wood was added; open circles did not receive experimental wood additions.

resistance based on a reanalysis of the dye transit data of Kaufmann (1987a). These data were taken mostly over a range of low to moderate flow stages revisited on 16 stream reaches, but include several storms and measurements near bankfull stage. The morphometric and hydraulic characteristics of these streams are shown in Table 1. Fig. 2A, plotted from data tabulated by Kaufmann (1987a), shows the moderately strong positive relationship between C_t and thalweg residual depth, expressed as a proportion of mean thalweg depth (both depths calculated from a long profile of bed elevation and water depth). Similarly, Fig. 2B and C, based on the same data source, show the stronger positive relationships between C_t and two other surrogates for topographic resistance or "form drag": the scaled standard deviations (i.e., CVs) of thalweg depth and the product of wetted width × thalweg depth. Fig. 2D shows the weaker positive relationship between C_t and in-channel wood volume alone expressed as a proportion of water depth (wood volume in reach divided by wetted channel volume). There is a stronger relationship between C_t and long-established in-channel wood volume (open circles) than with relatively recently added wood (solid circles in Fig. 2D). Newly added wood had an apparently lesser influence on C_t because its eventual influence by increasing channel scouring had not yet been realized (Kaufmann, 1987a). Fig. 2E shows a relationship between C_t and the summed relative submergence of residual depth plus wood that is similar in strength to that with the CV of the width-depth product (Fig. 2C).

To model the combined influences of wood, bedform roughness, and the relative submergence of these large-scale roughness features, we fit a regression predicting C_t from thalweg mean residual depth d_{res}, thalweg mean depth $d_{th,}$ and the sum of mean wood depth Wd and d_{res} from 36 data points where d_{res} was available ($R^2=0.77$, RMSE=0.18, $p<0.001$):

$$\mathrm{Log}C_t = 0.0835 + 1.08(\mathrm{Log}d_{\mathrm{res}}) + 0.638\mathrm{Log}[(d_{\mathrm{res}} + Wd)] - 3.32(\mathrm{Log}d_{\mathrm{th}}) \quad (13a)$$

Expressed in exponential form, this equation is:

$$C_t = 1.21 d_{\mathrm{res}}^{1.08}(d_{\mathrm{res}} + Wd)^{+0.638} d_{\mathrm{th}}^{-3.32} \quad (13b)$$

where $C_t=f_t/8$ is hydraulic resistance measured using dye transit experiments, and f_t is calculated using Eq. (3); d_{th} and d_{res} are, respectively, the thalweg mean depth and thalweg residual depth (m) from a long profile at 100 points along each stream reach, and Wd=mean wood "depth" (m) over the stream reach (wood volume/bankfull channel planform area). This model depicts hydraulic resistance as a decreasing function of the relative submergence of longitudinal bedforms and an interaction between large wood and bedforms. Fig. 2F shows the strength of Eq. (13a) in predicting C_t from channel morphology and wood in the data reported by Kaufmann (1987a).

We applied Eq. (13b) to the PNW Coast Range Ecoregion stream survey data set, which includes streams over a wider range of slope and size than those in the intensive dye-tracer study. We evaluated the validity of this application and the accuracy of C_t values calculated using Eq. (13b) in regional application by comparing discharges calculated using these C_t values with discharges measured on the same sampling date using velocity-depth methods (see Section 6.2). We caution that errors in predicting total resistance with this equation may result, in part, from not accounting for other sources of resistance (e.g, sinuosity, banks, vegetation, or width variation not highly correlated with depth).

5.4. Shields parameter

Values of the "Shields parameter" θ reported in the literature have been determined experimentally by relating shear stress to particle diameter at incipient motion and are often overestimated in natural stream conditions where form roughness is important (Buffington and Montgomery, 1999a; Parker et al., 2003). Buffington and Montgomery (1997) reviewed a wide range of incipient motion studies and reported θ values between 0.030 and 0.073 for rough, turbulent flows, based on laboratory flume studies using visual detection criteria for initial particle motion. The same authors reported θ values between 0.052 and 0.086 for laboratory and field-based studies using a reference transport rate to define initial motion. Rather than choosing a single representative value, we defined θ at incipient motion as a function of bankfull particle Reynolds number,

$$\mathrm{Re}_p = \left[(gR_{\mathrm{bf}}S)^{0.5} D_{\mathrm{gm}}\right]/v \quad (14)$$

based on a fit to the lower envelope of values in published empirical diagrams of θ versus Re_p, where v is the kinematic viscosity of water (1.02×10^{-6} m^2/s at 20 °C). For $\mathrm{Re}_p \le 26$, we defined θ according to our fit to the plot presented by Buffington and Montgomery (1997, plate 1):

$$\theta = 0.04\mathrm{Re}_p^{-0.24} \quad (15a)$$

For $\mathrm{Re}_p > 26$, we defined θ according to Parker et al. (2003), a modification of the formula of Brownlie (1981):

$$\theta = 0.5\left\{0.22\mathrm{Re}_p^{-0.6} + 0.06\left(10^{-7.7\mathrm{Re}_p^{-0.6}}\right)\right\} \quad (15b)$$

Shields numbers considerably higher than calculated by Eq. (15b) for high gradient streams (e.g., 0.13 to 0.20) were reported by Mueller et al. (2005) for streams with slopes of 5 to 10%, but the authors note that those θ values may have been elevated because of stabilizing bed structures or form drag on large particles not otherwise accounted for in their calculations. Our intention is to represent θ in our critical diameter calculation without the influence of form roughness, and then account for the effect of form roughness on critical diameter outside of the value of θ. Therefore, we use minimum θ to represent mobility under conditions with form roughness absent (see discussions by Buffington and Montgomery, 1997; Parker et al., 2003). The modeled relationship between θ and Re_p is shown in Fig. 3A, and its resultant relationship with D_{gm} in the PNW synoptic survey streams is illustrated in Fig. 3B. Streams with bed surface particles in the gravel to boulder range were assigned θ values from 0.022 to 0.030, those in the sand range θ values from 0.016 to 0.022, and silt-bedded streams values from θ =0.020 to 0.040.

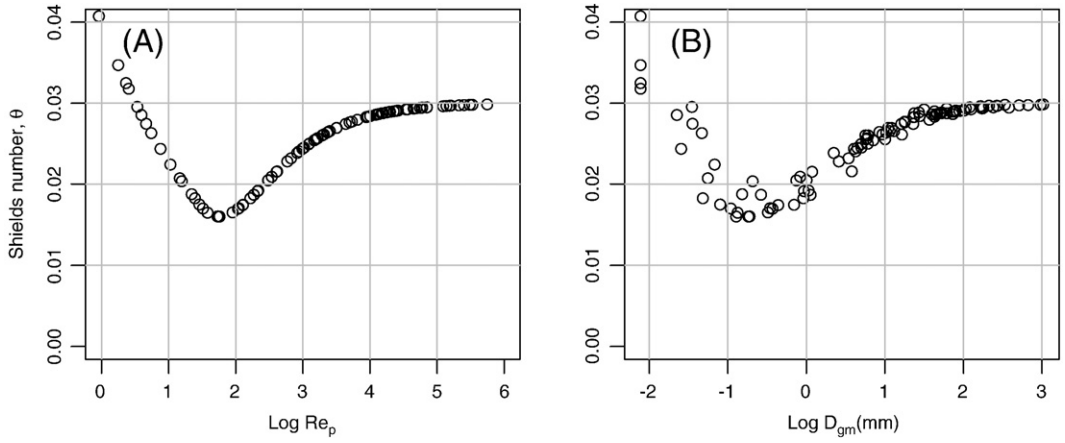

Fig. 3. Shields ratio at incipient motion, θ, applied in estimating D^*_{cbf} for 104 Oregon and Washington coastal streams sampled in 1994 and 1995, versus (A) Particle Reynolds Number, Log(Re_p), and (B) geometric mean bed surface particle diameter, LogD_{gm} in mm. Shields ratio was calculated as a function of particle Re_p at estimated bankfull flow conditions, based on the Equation of Parker et al. (2003) for $Re_p > 26$, and according to our fit to Buffington and Montgomery (1997, plate 1) for $Re_p \leq 26$.

5.5. Relative bed stability calculated from survey data

Finally, using the measure of effective hydraulic radius developed in Sections 5.2 and 5.3, $R^*_{bf} = R_p$ at bankfull flow = $R_{bf}(C_p/C_t)^{1/3}$, we modify the expression for RBS from Eq. (7) to accommodate reductions in shear stress exerted on the stream bed associated with large wood and longitudinal bedform roughness in sample reaches with lengths ~40 times their summer low flow wetted width:

$$\mathrm{RBS}^* = D_{gm}/D^*_{cbf} = D_{gm}/\left(0.604R^*_{bf}S/\theta\right) = 1.66\theta D_{gm}/\left\{R_{bf}\left(C_p/C_t\right)^{1/3}S\right\} \quad (16)$$

where:

D_{gm} = geometric mean bed surface particle diameter from systematic pebble counts (m);

D^*_{cbf} = bed surface particle critical diameter (m) at bankfull flow, averaged over reach, and adjusted for shear stress reductions due to wood and depth variation;

R_{bf} = bankfull hydraulic radius $\simeq 0.65 d_{th-bf}$, where d_{th-bf} = mean thalweg depth + bankful height above water surface (m);

R^*_{bf} = effective bankfull hydraulic radius (m) adjusted for wood and depth variation (Eq. (10b), setting $R^*_{bf} = R_p$ at bankfull flow);

S = energy slope ≃ slope of reach water surface, dimensionless ratio (m/m);

θ = shields number calculated from particle Reynolds number at bankfull flow $\{Re_p = [(gR_{bf}S)^{0.5}D_{gm}]/\nu\}$ using Eqs. (15a) and (15b);

C_p = stream reach-scale particle (grain) resistance at bankfull flow, calculated from reach wide mean relative submergence of D_{gm} using Eq. (12) with minimum $C_p = 0.002$; and

C_t = stream reach-scale total hydraulic resistance at bankfull flow, calculated from bankfull thalweg mean depth, thalweg mean residual depth, and wood volume per bankfull channel area using Eq. (13a). If calculated C_t was less than C_p, we set $C_t = C_p$.

For convenience and to homogenize its variance, we express RBS* values as logarithms in this paper, where LRBS* = Log_{10} [RBS*].

The calculation of bed particle size as the surface particle geometric mean diameter (D_{gm}) from EMAP pebble counts assumes log-linear particle size distribution within diameter classes. However, D_{gm} is more precise and repeatable than the D_{50} based on this coarse size class data (Faustini and Kaufmann, 2007), in which pebble count particle classifications were confined to seven diameter classes (see Section 3.1). We calculate the reach-average critical diameter (D^*_{cbf}) as shown above, using mean slope, bankfull height, thalweg mean depth, residual depth, and large wood volume per unit bankfull channel area, expressing all length measurements contributing to R^*_{bf} in SI units.

6. Test of RBS index on a regional survey data set

In this section, we show the results of applying the RBS* calculations to the PNW synoptic survey data. We examine the range of values, measurement precision, associations among hydraulic variables, and the response of RBS* to land disturbances that are thought to augment land erosion and sediment delivery to streams. Because of their importance in adjusting RBS* calculations for wood and channel form roughness, we also examine the accuracy or reasonableness of values obtained for the hydraulic resistance measure (C_t) when equations based on intensive dye tracer studies are applied to synoptic stream survey data that have a greater range in stream size and gradient.

6.1. General description of regional survey streams

The regional survey sites sampled in western Oregon and Washington are wadeable streams ranging from very small to large (bankfull width < 1 to ~50 m) at elevations near sea level

to almost 700 m (Table 2). Approximately 60% of channel slopes were >1%, although they ranged from <0.1 to 22%. Sinuosity of most of these channels was minimal (75% were <1.6), but ranged as high as 3.7. Field crews classified the majority of the survey reaches (*sensu* Montgomery and Buffington, 1997) as "pool riffle" channels (66%), with lesser numbers of "step-pool" (14%), "plane bed" (12%), and other (8%) channel types (e.g., "cascade," "braided," and not classified). The riparian margins of most of the study streams were heavily vegetated, though not always with large trees.

6.2. Reach-scale hydraulic resistance in regional survey streams

Bankfull values of C_t calculated using Eq. (13a) in the synoptic data set ranged from 0.002 to 1.68, with a median of 0.067 (Table 3), corresponding to Darcy Weisbach friction factor (f_t) values of 0.016 to 13.3, with a median of 0.54. Two of the 104 sites had values set to 0.002 as a result of calculated $C_t \leq C_p$. For low flow conditions, calculated C_t was higher (0.002 to 435) with a median approximately 28 times higher (1.9), corresponding to low flow f_t values of 0.016 to 3480 with a median of 15 (Table 3). Note that these were reach-scale values that included form resistance from pools and wood, and that some of the low flow values reflect very small discharges (e.g., <0.003 m^3/s). For comparison, Curran and Wohl (2003) measured f_t values ranging from 5 to 380 during low flows in 20 small step-pool channels containing woody debris; and in a related study, MacFarlane and Wohl (2003) reported values from 21 to 101 in 20 similar channels lacking woody debris. Beven et al. (1979) reported reach-average f_t values mostly between 1 and 48 for natural upland streams, with an extreme value of 1328.

Total resistance is expected to decline as discharge increases from low flow to bankfull conditions. Total resistance is a function of the size of roughness elements relative to flow depth (relative submergence), with roughness declining as flow depth and submergence increase (Wolman, 1955; Leopold and Wolman, 1957; Burkham and Dawdy, 1976; Bathurst et al., 1979). Curran (1999), for example, reported a decrease in f_t from 14 at summer low flow to 5 at bankfull flow in a small step-pool channel in the Washington Cascade Mountains. Similarly, Kaufmann (1987a) reported a change in f_t from 23 at low flow to 4 at near bankfull conditions in a small stream with abundant woody debris and complex pool-riffle morphology in the Oregon Coast Range. Systematic examination of hydraulic resistance in flume studies simulating step-pool channels with a range of wood volume, pool heights, wood and pool spacing, and grain resistances showed strong decreases

Table 2
Sample distributions of selected basin, channel, and riparian characteristics of 104 coastal stream reaches surveyed by the Oregon–Washington REMAP project, 1994–1995

Variable	Median	Range
Drainage area (km^2)	14	0.09–160
Q_{meas}=discharge at summer sample time ($m^3 s^{-1}$)	0.067	0–2.12
ELEV=elevation at sample reach (m)	121	3–673
S_s=mean slope of reach water surface (%)	1.2	0.08–22
Sinuosity of sample reach (m/m)	1.32	1.11–3.57
Mean bankfull width (m)	9.0	0.8–48
Mean wetted width (m)	5.6	0.38–23
d_{th-bf}=mean bankfull depth at thalweg (m)	1.1	0.27–2.6
SDd_{th}=Standard deviation of thalweg depth (m)	0.20	0.024–0.87
d_{res}=mean residual depth at thalweg (m)	0.17	0.0085–0.74
Mean total canopy cover over mid-channel (densiometer %)	78	13–100
Mean riparian tree+shrub+ground woody cover (%)	100	1.7–181
Mean riparian tree canopy cover (%)	40	0.8–89
Mean riparian tree canopy cover — trees>0.3 m dbh (%)	22	0–67
Riparian human disturb. — all types (prox-wt'd observ. per plot)	1.2	0–5.2
Riparian silvicultural disturb. (prox-wt'd observ. per plot)	0.38	0–1.5
Riparian road disturb. (prox-wt'd observ. per plot)	0.33	0–1.0
Riparian agricultural disturb. (prox-wt'd observ. per plot)	0.	0–2.1
Wd=large wood depth=(m^3 wood/m^2 bankfull channel area)	0.022	0–1.9
Large wood areal cover (% of wetted reach area)	7	0–58
RCOND=riparian condition index	0.47	0–0.92
WRCOND=watershed+riparian condition index	0.61	0–0.86

Table 3
Distributions of selected bed particle descriptors and calculated hydraulic characteristics of 104 coastal stream reaches surveyed by the Oregon–Washington REMAP Project, 1994–1995

Variable	Median	Range
Bed surface sand+fines (%≤2 mm diameter)	29	0–100
D_{gm}=bed surface particle geometric mean diameter (mm)	10	0.0077–1040
SDd_{th}/d_{th-bf}=coefficient of variation in bankfull thalweg depth	0.20	0.031–0.68
d_{res}/d_{th-bf}=bankfull mean residual depth proportion	0.16	0.00–0.40
Wd/d_{h-bf}=bkf. wood relative depth=(wood vol./channel area)/ d_{h-bf}	0.035	0.00–4.9
Re_p=bankfull particle Reynolds number	$10^{3.3}$	$10^{-0.04}$–$10^{5.8}$
θ=shields number at incipient motion (particle scale)	0.027	0.016–0.041
C_p=bankfull particle hydraulic resistance	0.0036	0.002–0.030
C_t=bankfull total hydraulic resistance (note $C_t=f_t/8$)	0.067	0.002–1.68
C_{t-low}=low flow total hydraulic resistance	1.9	0.002–435
C_p/C_t=ratio of particle/total hydraulic resistance at bankfull	0.067	0.0012–1.0
$(C_p/C_t)_{low}$=ratio of particle/total hydraulic resistance at low flow	0.002	0.00001–0.15
R_{bf}=bankfull total hydraulic radius (m)	0.71	0.18–1.7
R^*_{bf}=bankfull adjusted hydraulic radius (m)	0.35	0.02–1.7
R^*_{bf}/R_{bf}=ratio of adjusted/total bankfull hydraulic radius	0.41	0.11–1.0
D_{cbf}=bankfull critical diameter without adjustment (mm)	189	16–2600
D^*_{cbf}=bankfull critical diameter with adjustment (mm)	69	3.5–2100
D^*_{cbf}/D_{cbf}=ratio of adjusted/unadjusted bankfull critical diameter	0.41	0.11–1.0
LRBS_*bw5*=Log(Relative Bed Stability) fr. Kaufmann et al. (1999)	−0.70	−4.1–+1.2
LRBS*=Log(Relative Bed Stability)=Log[D_{gm}/D^*_{cbf}]	−0.87	−4.2–+0.98

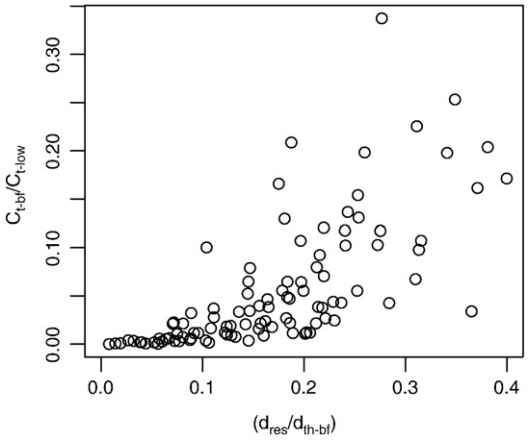

Fig. 4. Ratio of calculated total hydraulic resistance at bankfull flow to that at summer low flow (C_{t-bf}/C_{t-low}) versus relative residual depth at bankfull flow (d_{res}/d_{th-bf}), a measure of channel form roughness. Data are for 104 Oregon and Washington coastal streams sampled in 1994 and 1995.

in f_t with increasing discharge (Wilcox and Wohl, 2006). Our modeled decrease in C_t (or f_t) between low and bankfull flows follows these expected patterns, with a median ratio of bankfull/lowflow C_t of 3% with an interquartile range (IQR) of 1 to 8%. A high degree of complexity in channel morphology (e.g., large residual pool volume, abundant wood), however, tends to lessen the decline in resistance that occurs with increasing discharge in a given stream (Kaufmann, 1987a, Figs. 25 and 26). In the PNW synoptic data, modeled C_t differences between high and low flows were related to the degree of bedform roughness, as represented by bankfull residual pool relative roughness (d_{res}/d_{th-bf}) (Fig. 4). In streams with $d_{res}/d_{th-bf}<0.07$, bankfull C_t was a very small fraction (<1%) of low flow C_t, whereas in most streams with $d_{res}/d_{th-bf}>0.25$, bankfull C_t values were >10% of low flow C_t.

Comparison of C_t (from Eq. (13b)) with C_p (from Eq. (12)) illustrates the importance of form roughness (including "spill resistance") at the reach scale in the PNW synoptic survey of streams. Ratios of bankfull grain resistance to total resistance (C_p/C_t) ranged from 0.001 to 1.0, with a median of 0.067 (Table 3) and an IQR of 0.02 to 0.21. At low flow, the ratio ranged from 0.00001 to 0.15 with a median of 0.002 and an IQR of 0.0005 to 0.01. These model results are consistent with findings of Curran and Wohl (2003) who reported low flow grain resistance proportions from 0.0002 to 0.03 in complex step-pool channels with large woody debris (our calculation of f_g/f_t from their Table 3).

We further validated C_t estimates by comparing discharge values (Q_{calc}) calculated using C_t in Eq. (9a) with two types of independently measured discharge values. For flows lower than bankfull, we were able to directly compare Q_{calc} with 176 actual measurements of discharge using the velocity-area method (Q_{meas}) taken during summer (low) flows at the same time as channel morphology measures were collected during PNW synoptic surveys (104 stream reaches with 72 repeat visits at different times and flow conditions). The regression, $\text{Log}(Q_{calc}) = 0.264+1.002\text{Log}(Q_{meas})$, was highly significant ($p<0.0001$), with moderate precision ($R^2=0.80$ and RMSE=0.54) but some positive bias (Fig. 5). This is reasonable validation of the accuracy of C_t, but pertains to the low to moderate discharges measured during those surveys.

To evaluate the accuracy of our C_t estimates for bankfull conditions, we compared bankfull discharge estimates based on C_t and Eq. (9a) with the range of 1- to 2-year recurrence interval floods (scaled by drainage area) at gauged USGS sites in the same region. Castro and Jackson (2001) reported a median recurrence interval of 1.0 year (mean=1.2 year) for bankfull discharge in the PNW Maritime Mountain region that includes our study area. We compared our bankfull discharge estimates with the distribution of actual areal discharges for the one- and 1.4 year recurrence interval peak flows at 40 gauged stations (>20 years records) in the Oregon and Washington Coast Range within the basin size range of our study streams. The IQR of areal discharges (yield) for the 1.0- and 1.4-year floods were, respectively, 0.16 to 0.63 m^3s^{-1} km^{-2} and 0.25 to 0.98 $m^3s^{-1}km^{-2}$, with medians of 0.35 and 0.52 $m^3s^{-1}km^{-2}$ (Valerie Kelly, USGS, unpublished analysis of USGS data). These gauged areal discharges at or near bankfull conditions show good agreement with the distribution of bankfull areal discharges calculated for the 104 PNW synoptic survey streams using Eq. (9a) with field estimates of bankfull channel morphology and the C_t values from Eq. (13a) (IQR=0.18 to 0.93, with a median of 0.34 $m^3s^{-1}km^{-2}$).

In summary, although our C_t estimates are higher than might be expected based on values reported in the literature (which pertain mostly to riffle cross sections or shorter reaches), they

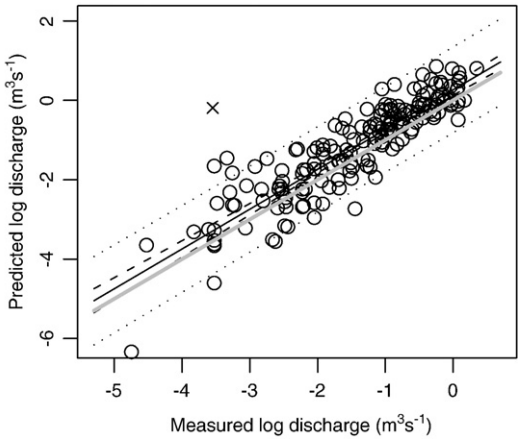

Fig. 5. Calculated discharge, $\text{Log}(Q_{calc})$ in m^3s^{-1}, based on low flow channel measurements applied to Eq. (9a) ($Q=(1/C_t)^{1/2}A_{xs}(gRS)^{1/2}$), versus discharge measured on the same day using the velocity-area method, $\text{Log}(Q_{meas})$ in m^3s^{-1}. Channel measurements contributing to Eq. (9a) included total hydraulic resistance C_t, channel water surface gradient, mean flow cross-sectional area, and mean hydraulic radius. C_t here pertains to sampled (not bankfull) conditions, and is based on measurements of thalweg mean depth d_{th}, thalweg mean residual depth d_{res}, and large wood volume per bankfull channel area, Wd, applied to Eq. (13a). Data are from a survey of PNW coastal streams sampled in 1994–1996 (104 stream reaches with 72 repeat visits at different times and flow conditions). The regression, shown as a solid line with 95% confidence bounds on the mean and individual observations, was $\text{Log}(Q_{calc})=0.264+1.002\text{Log}(Q_{meas})$. The regression was highly significant ($p<0.0001$), with moderate precision ($R^2=0.80$ and RMSE=0.54), but some positive bias. The X symbol shows site not included in regression, with 100% combined areal cover of aquatic macrophytes and brush, two roughness types not well represented in the calculation of C_t. The line of perfect agreement (1:1) is shown in gray.

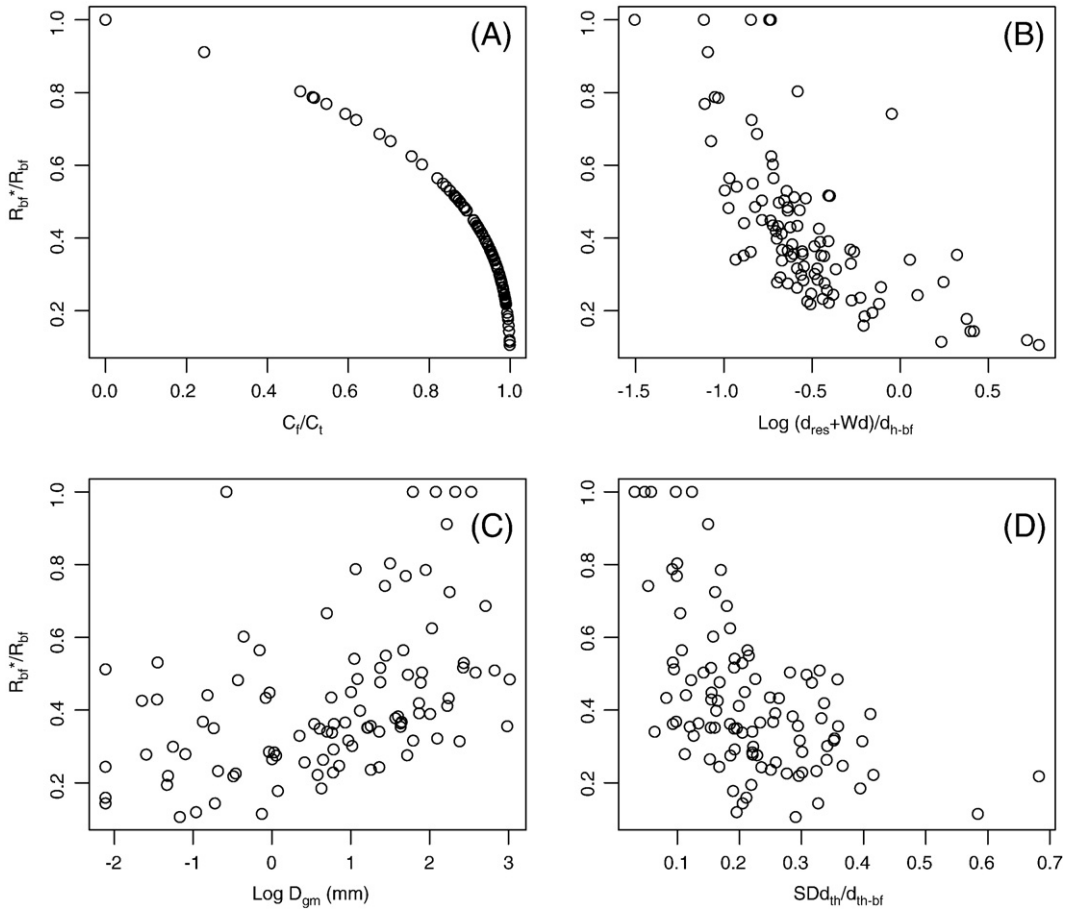

Fig. 6. Ratio of adjusted to unadjusted bankfull hydraulic radius (R^*_{bf}/R_{bf}) versus (A) ratio of bankfull form resistance to total hydraulic resistance, $C_f/C_t = 1-(C_p/C_t)$; (B) combined relative roughness of wood and residual pools ($d_{res}+Wd)/d_{h-bf}$; (C) geometric mean particle surface diameter, D_{gm}, log transformed; and (D) relative thalweg depth variation at bankfull flow (SDd_{th-bf}/d_{th-bf}).

are similar to recently reported reach-scale measurements of hydraulic resistance in natural streams with relatively complex morphology. In addition, discharges predicted using our C_t values with reach-scale measures of channel morphology agree well with measured discharges taken at the same time in the study streams, and corroborate well with the expected range in the magnitude of areal bankful discharges in the region. Further, comparison of C_t with C_p suggests that form roughness generally dominates particle roughness in these streams, even at bankfull conditions (Table 3). These results suggest two things: (i) that roughness other than that resulting from bed surface particles is of sufficient magnitude in PNW coastal streams and probably in most other regions to necessitate its consideration in calculations of shear stress exerted on bed surface particles, and (ii) that our estimates of total hydraulic resistance are sufficiently accurate (or at least plausible) for use in adjusting hydraulic radius based on C_p/C_t in our formulation of RBS*.

6.3. Hydraulic radius adjustments in regional survey streams

The ranges of reach mean hydraulic radius estimates were 0.18–1.7 m for unadjusted R_{bf} and 0.02–1.7 m for adjusted R^*_{bf} in the PNW synoptic sample (104 stream reaches). The median value for the ratio R^*_{bf}/R_{bf} was 0.41 in these streams (Table 3), with an interquartile range of 0.28 to 0.59, showing a moderate amount of downward adjustment of R_{bf} as a result of modeling R^*_{bf} using the hydraulic resistance ratio discussed in the previous section, where $R^*_{bf}=R_{bf}(C_p/C_t)^{1/3}$. This modeled relationship is illustrated in Fig. 6A, in which we have plotted R^*_{bf}/R_{bf} as a function of the form resistance ratio C_f/C_t, where we have defined $C_f=(C_t-C_p)$ and $C_f/C_t=[1-(C_p/C_t)]$ to illustrate more clearly the modeled effect of form resistance on the hydraulic radius adjustment. Fig. 6A shows that adjustment of the hydraulic radius remains <50% (i.e., $R^*_{bf}/R_{bf}>0.50$) until form resistance comprises more than ~85% of total hydraulic resistance, beyond which R^*_{bf}/R_{bf} declines steeply. Interestingly, R^*_{bf}/R_{bf} declines approximately log-linearly with the combined relative roughness (height) of residual pools plus large wood until a relative roughness of ~0.5, or a log relative roughness of −0.3), and then declines more slowly at higher relative roughness (Fig. 6B). The ratio R^*_{bf}/R_{bf} generally increases with D_{gm}, (i.e., smaller R^*_{bf} adjustments) because of the influence of particle size on the ratio of particle to form resistance (C_p/C_t), as illustrated in Fig. 6C. Conversely, R^*_{bf}/R_{bf} generally decreases with bankfull thalweg depth variation (SDd_{th-bf}/d_{th-bf}), as illustrated in Fig. 6D, because

thalweg depth variation is one of the major contributors to estimation of total hydraulic resistance in the ratio C_p/C_t.

6.4. Precision of LRBS* and related measurements

The RMS_{rep} of a variable quantifies the average variation in its measured value between same-season site revisits, pooled across all sites where measurements were repeated. The RMS_{rep} of LRBS* = 0.44, or 8.6% of its observed range among sites (Table 4). Similarly, the RMS_{rep} values for Log[D_{gm}], Log[D^*_{cbf}] and R^*_{bf} were 0.43 (Log-mm), 0.26 (Log-mm), and 0.12 m; and these were, respectively, 8.3, 9.2 and 7.7% of their observed ranges in the region. The ratio of LRBS* variance among sample streams divided by the LRBS* variance for same-year revisits (i.e., replicate samples) within streams, a "signal/noise ratio," was 5.6. This degree of relative precision indicates moderate potential for discriminating among sites and detecting correlations between LRBS* and potential controlling variables in this region (Kaufmann et al., 1999). In the last column of Table 4, we show the computed changes in LRBS* that would result from a 1 RMS_{rep} increase in each of its subcomponent variables. Among the primary measurement variables contributing to and limiting the precision of LRBS* in the PNW Coastal stream survey, the precision of D_{gm} appears to be the dominant limitation. A 1 RMS_{rep} increase in D_{gm} results in an LRBS* increase of ~8% of the range of LRBS* in the study region. The measurement variability of D_{gm} is followed in rank order of importance by that for the estimates of S, Wd, R_{bf}, and d_{res}, which combine through calculation of C_p/C_t, R^*_{bf}/R_{bf}, Re_p and θ to calculate D^*_{cbf}. Although the RMS_{rep} of S is relatively independent of the magnitude of S, its effect on LRBS* is not, because it appears in multiplication of the depth-slope product. This variable effect is shown by the range of effects on LRBS* shown for S in the last column of Table 4. The effect of a 1 RMS_{rep} increase in S would cause a decrease in LRBS* of −0.21 in streams with S = 0.005, but only −0.06 and −0.03 for streams with S = 0.02 and 0.04, respectively. Of the primary measurement variables contributing to LRBS*, only D_{gm} and S have sufficient imprecision to affect LRBS* by more than 0.1, which is approximately 2% of the range of LRBS* in the study region.

6.5. Bed surface particle size and stability

Geometric mean bed surface particle diameters (D_{gm}) in the PNW Coastal Ecoregion study reaches ranged from silt to very large boulders. Values of LRBS* ranged from −4.2 to +0.98 (a range of five orders of magnitude), with a median of −0.87 (Table 3). The IQR of LRBS* was −2.0 to −0.24, showing that D_{gm} was finer than D^*_{cbf} in most streams. In fact, only 16% of the sample streams had D_{gm} coarser than D^*_{cbf}. The median value of the ratio of adjusted to unadjusted critical diameters (D^*_{cbf}/D_{cbf}) was 40% (IQR of 28–59%). In those streams with abundant large wood and complex channel morphology, D^*_{cbf} was as low as 11% of the unadjusted D_{cbf}, illustrating the dominant role that these large-scale roughness features can play in dissipating shear stresses that otherwise would be exerted in mobilizing the streambed.

Table 4
Precision of LRBS* and its subcomponent variables calculated from 29 same-season revisits allocated to 19 sites during the sampling of 104 coastal stream reaches surveyed in 1994–1996 by the Oregon–Washington REMAP Project

Variable	Mean	RMS_{rep}	S/N	LRBS* Chg for 1 RMS_{rep} increase
Primary measurement variables:				
Log[D_{gm}] = Log[bed surface particle geometric mean diameter, mm]	0.80	0.43	8.3	+0.43
R_{bf} = bankfull total hydraulic radius (m)	0.68 m	0.11 m	6.3	−0.07
Log[d_{res}] = Log(residual depth, m)	−0.88	0.071	28.1	+0.04
Log[Wd] = Log[wood vol./bankfull channel surface area, m^3/m^2]	−1.77	0.40	4.1	+0.09
S = mean slope of reach water surface	0.021	0.0032	74.3	−0.06 (−0.21 to −0.03)
Derived variables:				
Log[C_p] = Log[bankfull particle hydraulic resistance coefficient]	−2.37	0.12	6.1	−0.04
Log[C_t] = Log(bankfull total hydraulic resistance coefficient]	−1.22	0.30	2.3	+0.07
C_p/C_t = ratio of particle/total hydraulic resistance at bankfull	0.18	0.14	2.0	−0.05
R^*_{bf}/R_{bf} = ratio of adjusted/total bankfull hydraulic radius	0.46	0.12	2.7	−0.04
R^*_{bf} = bankfull adjusted hydraulic radius (m)	0.34 m	0.12 m	3.9	−0.13
Log[Re_p] = Log[bankfull particle Reynolds number]	3.22	0.45	8.6	+0.01
θ = shields number at incipient motion (particle scale)	0.024	0.0022	4.0	+0.04
Log[D^*_{cbf}] = Log[bankfull critical diameter with adjustment, mm]	1.86	0.26	3.1	−0.26
Final calculation:				
LRBS* = Log(relative bed stability) = Log[D_{gm}/D^*_{cbf}]	−1.06	0.44	5.6	+0.44

RMS_{rep} is the root-mean-square error of repeat visits during the same year, a measure of the precision or replicability of field measurements, equivalent to the root-mean-square error (RMSE) relative to the site means (e.g., as applied by Kaufmann et al., 1999). S/N is the ratio of variance among streams to that in repeat visits to the same stream. LRBS* change is the computed change in the value of LRBS* that would result if each specified variable were increased by 1 × RMS_{rep} above its mean. (Because the effect on LRBS* of a 1 RMS_{rep} change in S is strongly inversely related to the magnitude of S, the LRBS* change is shown in parenthesis for S = 0.005 and S = 0.04).

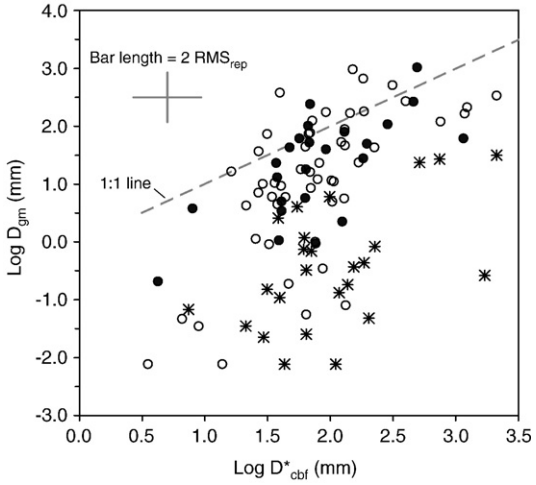

Fig. 7. LogD_{gm} vs Log$D*_{cbf}$ in 104 Oregon and Washington coastal streams sampled in 1994 and 1995, showing three levels of basin-riparian disturbance (data from first visit only). Solid circles are sites with the least amount of streamside human land disturbances, the most dense and multi layered corridor of woody riparian vegetation, and the lowest basin road densities (RCOND > 0.6, WRCOND > 0.6, and Rd_Denkm < 2.0 km/km^2). Stars are sites with high amounts of human riparian and basin disturbance (i.e., RCOND < 0.4, WRCOND < 0.5 and Rd_Denkm > 2.8 km/km^2). Remaining (medium disturbance) sites are shown as open circles. Length of error bars = 2(RMS$_{rep}$), where RMS$_{rep}$ for LogD_{gm} and Log$D*_{cbf}$ are, respectively, 0.43 and 0.27. Dashed line represents $D_{gm} = D*_{cbf}$ (and consequently LRBS* = 0).

6.6. Factors controlling bed surface particle size and stability

When streams of all disturbance classes were taken together, observed bed surface particle diameter (D_{gm}) and critical diameter ($D*_{cbf}$) were only weakly correlated (all data points in Fig. 7). To examine this relationship in relatively undisturbed streams and to assess the influence of human activities on this relationship, we divided streams into three disturbance categories. We used progressive degrees of riparian disturbance and basin road density as a proxy for levels of sediment supply from erosion and mass wasting. The subset of 24 least-disturbed stream reaches are shown as filled circles in Fig. 7. These sites had the least amount of streamside human land disturbances, the most dense and multi-layered corridor of woody riparian vegetation, and the lowest basin road densities (RCOND ≥ 0.6, WRCOND ≥ 0.6, and Rd_Denkm < 2.0 km/km^2). Over a range of nearly three orders of magnitude in $D*_{cbf}$, observed bed surface particle diameter (D_{gm}) was generally within an order of magnitude of critical diameter ($D*_{cbf}$) in this subset of 24 lesser-disturbed streams. (Streams with $D_{gm} = D*_{cbf}$ would fall along the diagonal 1:1 line in the figure and would have LRBS* = 0.) LRBS* ranged from −1.9 to +0.5 in these 24 lesser-disturbed streams with a median of −0.44 (IQR −1.06 to −0.16). By contrast, streams with high amounts of human riparian and basin disturbances (i.e., RCOND < 0.4, WRCOND < 0.5, and Rd_Denkm > 2.8 km/km^2) typically fell well below the 1:1 line (star symbols in Fig. 7), indicating that they had lower LRBS* than that observed in less disturbed streams. LRBS* ranged from −4.2 to −1.1 in these 25 most-disturbed streams, with a median of −2.43 and IQR of −2.95 to −1.83. Streams with intermediate disturbance (open circles) were sometimes well below the 1:1 line on Fig. 7, but unlike those with high disturbance, they also substantially overlapped the distribution of low disturbance streams.

Although we do not stress individual site assessments in this article, the survey measurements can be used for this purpose with due consideration of measurement precision. For example, the magnitude of individual site variation in D_{gm} and $D*_{cbf}$ are shown by the error bars (each 2SD$_{rep}$ or 2RMS$_{rep}$) in Fig. 7. An elipse surrounding the vertical and horizontal error bars describes the expected confidence of the numerator and the denominator of LRBS* at any individual site. The magnitude of LRBS* at each site in Fig. 7 is shown by its displacement above or below the 1:1 line, and the error bounds for D_{gm} and $D*_{cbf}$ give a visual indication of the magnitude of individual LRBS* differences that can be considered different. For example, individual site values of D_{gm} that are 2 orders of magnitude lower than $D*_{cbf}$ (ie., those that have LRBS* ≤ 2.0) can be clearly interpreted to be lower than those with LRBS* ≥ 0.0. The fact that all of the sites with the greatest amount of basin and riparian anthropogenic disturbance have D_{gm} one to four orders of magnitude smaller than $D*_{cbf}$ strongly suggests anthropogenic disturbance may be considered a possible cause.

The progressive decline in LRBS* in streams across five classes of increasing anthropogenic basin and riparian disturbance in the PNW coastal region is shown in Fig. 8. Although it may be unclear whether there is substantial difference in the central tendency of LRBS* among disturbance levels 1 to 3, it is clearly evident that LRBS* is systematically lower at the two highest disturbance levels (DISTLEVEL 4 and 5). LRBS* varies widely at intermediate disturbance levels, but there is virtually no overlap between the least and most disturbed streams. The least disturbed streams (DISTLEVEL 1) have LRBS* mostly between −1.0 and 0.0, while most of the highly-disturbed streams (DISTLEVEL 5) have LRBS* between −3.4 and −2.4. These data show that low values of LRBS* in this region are

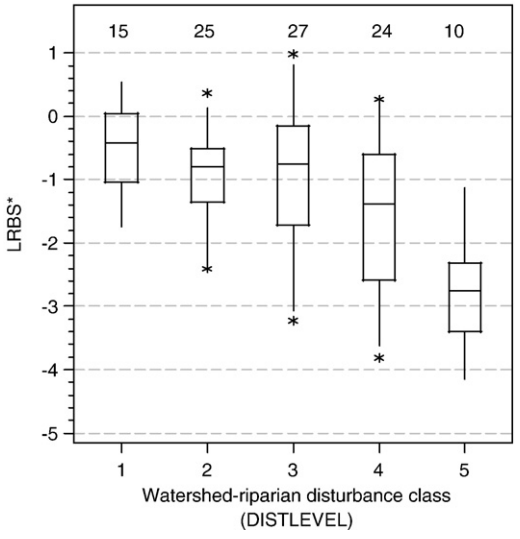

Fig. 8. LRBS* vs watershed-riparian disturbance class (DISTLEVEL) in 104 Oregon and Washington coastal streams sampled in 1994 and 1995; box and whisker plot shows median, 25th and 75th percentiles, 5th and 95th percentiles.

associated with human disturbance, but do not in themselves show the degree to which these low values result from streambed "fining" (sedimentation) as opposed to increases in bed shear stress (e.g., see discussions by Millar and Rennie, 2001; Wilcock, 2001).

7. Generality of results and remaining uncertainties

We developed an index of relative bed stability for wadeable streams, RBS*, that explicitly takes into account the reduction in shear stress on bed particles resulting from the large scale roughness of pools and large wood. RBS* should be calculated over relatively long stream reaches (e.g., 40 times mean wetted width) and requires estimates of bed surface particle size (D_{gm} or D_{50}), water surface gradient, mean bankfull channel dimensions, large wood volume, and separate estimates of particle-scale ("grain") and total hydraulic resistance at bankfull stage. For regional assessments, we demonstrate that these can be adequately obtained from a systematic visually classified pebble count, a thalweg depth profile, 11 bankfull channel dimension transects, and a channel reach slope sighting, as measured by field surveyors using relatively coarse field protocols such as that used by the USEPA in the EMAP surveys (see Peck et al., 2006; available at: http://www.epa.gov/emap/html/pubs/doc/groupdocs/surfwatr/field/ewwsm01.html; accessed in October, 2006). Despite the coarse nature of data collection compared with many research efforts, the LRBS* index calculated from these synoptic survey data appears to have sufficient range and precision to be a useful measure of bed stability across the wide range of stream sizes, slopes, and locations in this synoptic survey of streams, and to reveal associations between bed stability and land use disturbance in the PNW Coastal Ecoregion. Our results show a substantial degree of bed textural fining (lower-than-expected LRBS*) in streams draining watersheds that have high basin road density, high streamside human land use activity, and low cover and complexity of riparian vegetation. Reductions in the amount, structural complexity, and mechanical stability of riparian vegetation reduce the effectiveness of riparian corridors in physically trapping sediment, stabilizing long-term sediment storage in stream banks and valley bottoms, and in supplying large wood that dissipates shear stresses that would otherwise transport sediment (Gregory et al., 1991; Maser and Sedell, 1994). The negative association of LRBS* with basin road density and riparian human disturbances in this region suggests that human activities may have either augmented erosion and decreased riparian buffering, leading to accumulation of fines in streambeds, and/or increased bed shear stress resulting from hydrologic alteration or reductions in bed roughness. In streams with low LRBS*, bed materials are easily moved by floods smaller than bankfull, so may be rapidly transported downstream. The persistence of fine particles in these streambeds under these circumstances can only be made possible by rates of sediment supply (including fines) that are sufficient to continue to replenish the streambed. In contrast, low LRBS* resulting from hydrologic alterations that increase bed shear stress would likely be less persistent, because (assuming the availability of coarse bed material) streambed armoring would rapidly stabilize the bed by increasing D_{gm}, thereby also increasing LRBS*.

Some modifications in field measurements would improve their utility for assessing RBS* in regional assessments. Peck et al. (2006) increased the bed particle count from 55 to 105 particles (5 particles in each of 21 cross sections), required two survey rods for the measurement of clinometer slope, and provided more comprehensive guidance and field crew training in estimating bankfull height, particle sizes, and slope for the EMAP surveys. These improvements resulted in a reduction of the RMS_{rep} for $Log[D_{gm}]$ from 0.43 in the survey discussed in this article to 0.21–0.27 in more recent EMAP surveys (Stoddard et al., 2005a,b; Faustini and Kaufmann, 2007). The precision of $Log[D^*_{cbf}]$ remained about the same, 0.27 compared with 0.26 in the earlier survey. The field modifications yielded somewhat more precise measures of relative bed stability. For example, the RMS_{rep} of LRBS* in the more recent surveys was 0.40 with an among/within stream variance ratio (signal/noise) of 7, compared with values of $RMS_{rep}=0.44$ and signal/noise variance ratio of 5.6 in the earlier survey we examined here. The modified procedures have somewhat greater potential to detect trends and assess sedimentation than those used in the earlier surveys described in this article, and whose trend detection capabilities were reported by Larsen et al. (2004).

Our results suggest that the LRBS* index applied to synoptic survey methods and designs like those used by EMAP are adequate to evaluate regional patterns in bed stability and its general relationship to human disturbances. Although the RBS* concept itself also shows promise for evaluating bed stability in individual streams, our approach is relatively coarse, and site-specific assessments using these relatively rapid field methods might prudently be confined to identifying severe cases of altered bed stability resulting from alteration of sediment supply, discharge, or channel morphology. Greater confidence in site-specific assessments could be gained by calculating RBS* using more precise field measurements of channel slope and bed particle size, and by refining and further validating the calculations for bed shear stress reduction resulting from channel form roughness, including wood, cross-section variation, pools, and other sources of resistance such as banks and sinuosity not explicitly modeled in our equations. The precision and accuracy of D_{gm} measurements are a major limitation of the precision of RBS* using the field techniques employed in the surveys we describe. Substantial improvement was gained by better training and increasing the number of particles from 55 to 105 in recent surveys. However, D_{gm} precision could be further improved by monumenting the reach location and fixing the reach length between revisits to the same reach, by increasing the number of bed particles size classes from 6 to 12, and by employing templates or rulers to assign particles to size classes (Faustini and Kaufmann, 2007). Use of a roofer's water (hydrostatic) level or a laser level would improve slope measurement precision, especially on slopes $<1.5\%$, below which slope measurement imprecision begins to limit the precision of RBS* (see Table 4). Further hydraulic research to quantify form resistance at bankfull conditions would probably be required to

improve the RBS* adjustment for large-scale roughness. Finally, we encourage research to test the RBS* concept in a wider variety of geomorphic settings, using more rigorous and accurate field methods, and exploring alternative approaches for accommodating the effects of additional sources of hydraulic resistance.

Acknowledgements

The research presented in this manuscript was undertaken at the U.S. EPA's Western Ecology Division of the National Health and Environmental Effects Laboratory in Corvallis, OR, funded by the USEPA through the Environmental Monitoring and Assessment Program (EMAP), its Regional (R-EMAP) surveys, and a Regional Methods Initiative grant from the EPA Office of Water. Hydraulic dye transport data were collected and analyzed by the lead author in 1983–1986, with Ph.D. research support from the OSU Dept. of Forest Engineering and a fellowship from the Weyerhauser Corporation. We are grateful for the use of Oregon and Washington synoptic survey data collected and made available to us through cooperation with Glen Merritt, Rick Hafele, Mike Mulvey, Lil Herger, and Gretchen Hayslip. We are also grateful to Curt Seeliger and Marlys Cappaert for data management and validation, Sue Pierson for map preparation, and Val Kelly for regional flood frequency analyses. We thank John VanSickle, Alan Herlihy, David Peck, and Colleen Birch-Johnson for advice on data analysis and we are grateful to John Stoddard, Steve Paulsen, Margaret Passmore, and Gretchen Hayslip for funding and program support. We thank Dave Montgomery, John Buffington, Brian Bledsoe, Peter Wilcock, John Potyondy, and Bob Beschta for enlightening discussions of sediment transport concepts, and John VanSickle and two anonymous reviewers for comments on earlier drafts. This manuscript has been subjected to review by the National Health and Environmental Effects Research Laboratory's Western Ecology Division and approved for publication. Approval does not signify that the contents reflect the views of the Agency, nor does mention of trade names or commercial products constitute endorsement or recommendation for use.

References

Bathurst, J.C., 1981. Discussion of 'bar resistance of gravel-bed streams'. J. Hydraul. Div., ASCE 107, 1276–1278.

Bathurst, J.C., Li, R.M., Simons, D.B., 1979. Hydraulics of Mountain Rivers. Colorado State University Experiment Station Report CER78–79JCB-RML DB55, Fort Collins.

Beven, K., Gilman, K., Newson, M., 1979. Flow and flow routing in upland channel networks. Hydrol. Sci. Bull. 24 (3), 303–325.

Bledsoe, B.P., Watson, C.C., 2001. Logistic analysis of channel pattern thresholds: meandering, braiding, and incising. Geomorphology 38, 281–300.

Bledsoe, B.P., Brown, M.C., Raff, D.A., 2007. Geotools: a toolkit for fluvial system analysis. JAWRA 43 (3), 757–772.

Brownlie, W.R., 1981. Prediction of Flow Depth and Sediment Discharge in Open Channels. Rep. No. KH-R-43A, W.M. Deck Laboratory of Hydraulics and Water Resources. California Institute of Technology, Pasadena.

Buffington, J.M., 1995. Effects of hydraulic roughness and sediment supply on surface textures of gravel-bedded rivers. M.S. Thesis, Dept of Geological Sciences, University of Washington, Seattle.

Buffington, J.M., 1998. The use of streambed texture to interpret physical and biological conditions at watershed, reach, and sub-reach scales. Ph.D. Dissertation, Dept. of Geological Sciences, University of Washington, Seattle.

Buffington, J.M., Montgomery, D.R., 1997. A systematic analysis of eight decades of incipient motion studies, with special reference to gravel-bedded rivers. Water Resour. Res. 33 (8), 1993–2029.

Buffington, J.M., Montgomery, D.R., 1999a. Effects of hydraulic roughness on surface textures of gravel-bed rivers. Water Resour. Res. 35 (11), 3507–3521.

Buffington, J.M., Montgomery, D.R., 1999b. Effects of sediment supply on surface textures of gravel-bed rivers. Water Resour. Res. 35 (11), 3523–3530.

Buffington, J.M., Montgomery, D.R., 2001. Reply to comments by Wilcock and by Millar and Rennie on "Effects of hydraulic roughness on surface textures of gravel-bed rivers". Water Resour. Res. 37 (5), 1529–1533.

Burkham, D.E., Dawdy, D.R., 1976. Resistance equation for alluvial-channel flow. J. Hydraul. Div., ASCE 102 (HY10), 1479–1489.

Calkins, D., Dunne, T., 1970. A salt tracing method for measuring channel velocities in small mountain streams. J. Hydrol. 11, 379–392.

Castro, J.M., Jackson, P.L., 2001. Bankfull discharge recurrence intervals and regional hydraulic geometry relationships: patterns in the Pacific Northwest, U.S.A. J. Am. Water Resour. Assoc. 37 (5), 1249–1262.

Cowan, W.L., 1956. Estimating hydraulic roughness coefficients. Agric. Eng. 37, 473–475.

Chow, V.T., 1959. Open Channel Hydraulics. McGraw-Hill, New York.

Curran, J.H., 1999. Hydraulics of large woody debris in step pool channels, Cascade Range, Washington. M.S. Thesis, Colorado State University, Fort Collins.

Curran, J.H., Wohl, E.E., 2003. Large woody debris and flow resistance in step-pool channels, Cascade Range, Washington. Geomorphology 51, 141–157.

Dietrich, W.E., Kirchner, J.W., Ikeda, H., Iseya, F., 1989. Sediment supply and the development of the coarse surface layer in gravel bed rivers. Nature 340 (20), 215–217.

Dingman, S.L., 1984. Fluvial Hydrology. W.H. Freeman, New York.

Einstein, H.A., Barbarossa, N.L., 1952. River channel roughness, Trans. ASCE 117, 1121–1132.

Emmett, W.W., Wolman, M.G., 2001. Effective discharge and gravel-bed rivers. Earth surf. processes landf. 26 (13), 1369–1380.

Engelund, F., 1966. Hydraulic resistance of alluvial streams. Proc. Am. Soc. Civil Eng. 92, 315–326.

Faustini, J.M., Kaufmann, P.R., 2007. Adequacy of visually classified particle count statistics from regional stream habitat surveys. J. Am. Water Resour. Assoc. 43 (5), 1293–1315. doi:10.1111/j.1752–1688.2007.00114.x.

Gordon, N.D., McMahon, T.A., Finlayson, B.L., 1992. Stream Hydrology, An Introduction for Ecologists. Wiley, New York.

Gregory, S.V., Swanson, F.J., McKee, W.A., Cummins, K.W., 1991. An ecosystem perspective of riparian zones. Bioscience 41, 540–551.

Herger, L., Hayslip, G., 2000. Ecological condition of streams in the Coast Range ecoregion of Oregon and Washington. EPA/910/R-00/002. U.S. Environmental Protection Agency, Region 10, Seattle, WA.

Herlihy, A.T., Larsen, D.P., Paulsen, S.G., Urquhart, N.S., Rosenbaum, B.J., 2000. Designing a spatially balanced, randomized site selection process for regional stream surveys: the EMAP Mid-Atlantic pilot study. Environ. Monit. Assess. 63, 95–113.

Hey, R.D., 1979. Flow resistance in gravel-bed rivers. J. Hydraul. Div., ASCE 104 (6), 869–885.

Howard, A.D., 1980. Thresholds in river regimes. In: Coates, D.R., Vitek, J.D. (Eds.), Thresholds in Geomorphology. George Allan and Unwin, Boston, MA, pp. 227–258.

Hubbard, E.F., Kilpatrick, F.A., Martens, L.A., Wilson Jr., J.R., 1982. Measurement of time of travel and dispersion in streams by dye tracing. Techniques of Water Resources Investigations of the U.S. Geologic Survey. USGS, Alexandria, VA. Chapter A9.

Hughes, R.M., Howlin, S., Kaufmann, P.R., 2004. A biointegrity index for coldwater streams of western Oregon and Washington. Trans. Am. Fish. Soc. 133, 301–312.

Jarret, R.D., 1984. Hydraulics of mountain streams. J. Hydraul. Div., ASCE 110, 1519–1539.

Jowett, I.G., 1989. River Hydraulic and Habitat Simulation, RHYHABSIM computer manual. N.Z. Fish. Misc. Rep., vol. 49. Christchurch, New Zealand.

Kappesser, G., 2002. A riffle stability index to evaluate sediment loading to streams. J. Am. Water Resour. Assoc. 38 (4), 1069–1081.
Katul, G., Wiberg, P., Albertson, J., Hornberger, G., 2002. A mixing layer theory for flow resistance in shallow streams. Water Resourc. Res. 11, 1250. doi:10.1029/2001WR000817.
Kaufmann, P.R., 1987a. Channel morphology and hydraulic characteristics of torrent-impacted forest streams in the Oregon Coast Range, U.S.A., Ph.D. Dissertation, Dept. of Forest Engineering/Hydrology, Oregon State University, Corvallis.
Kaufmann, P.R., 1987b. Slackwater habitat in torrent-impacted streams. In: Beschta, R.L., Blinn, T., Grant, G.E., Swanson, F.J., Ice, G.E. (Eds.), Erosion and Sedimentation in the Pacific Rim. International Association of Hydrologic Science, Pub. No. 165, Proceedings of an International Symposium, August 3–7, 1986. Oregon State Univ., Corvallis, pp. 407–408.
Kaufmann, P.R., Hughes, R.M., 2006. Geomorphic and anthropogenic influences on fish and amphibians in Pacific Northwest coastal streams. In: Hughes, R.M., Wang, L., Seelbach, P.W. (Eds.), Landscape Influences on Stream Habitats and Biological Assemblages. American Fisheries Society Symposium, vol. 48. Bethesda, Maryland, pp. 429–455.
Kaufmann, P.R., Robison, E.G., 1998. Physical habitat characterization. In: Lazorchak, J.M., Klemm, D.J., Peck, D.V. (Eds.), Environmental Monitoring and Assessment Program—Surface Waters: Field Operations and Methods for Measuring the Ecological Condition of Wadeable Streams. EPA/620/R-94/004F. U. S. Environmental Protection Agency, Office of Research and Development, Washington, D.C., pp. 77–118. Available at http://www.epa.gov/emap/html/pubs/docs/groupdocs/surfwatr/field/ws_abs.html. Accessed in October 2006.
Kaufmann, P.R., Levine, P., Robison, E.G., Seeliger, C., Peck, D.V., 1999. Quantifying Physical Habitat in Wadeable Streams. EPA/620/R-99/003. U.S. Environmental Protection Agency, Washington, DC. Available at http://www.epa.gov/emap/html/pubs/docs/groupdocs/surfwatr/field/phyhab.html. Accessed in October 2006.
Keim, R.F., Skaugset, A.E., 2002. Physical aquatic habitat. I. Errors associated with measurement and estimation of residual pool volumes. N. Am. J. Fish. Manag. 22, 145–150.
Keim, R.F., Skaugset, A.E., Bateman, D.S., 2002. Physical aquatic habitat II. Pools and cover affected by large woody debris in three western Oregon streams. N. Am. J. Fish. Manag. 22, 151–164.
Keulegan, G.H., 1938. Laws of turbulent flow in open channels. J. Natl. Bur. Stand. 21, 707–741.
Lane, E.W., 1955. The importance of fluvial morphology in hydraulic engineering. Proc. ASCE. 81 (745), 1–17.
Larsen, D.P., Kaufmann, P.R., Kincaid, T.M., Urquhart, N.S., 2004. Detecting persistent change in the habitat of salmon-bearing streams in the Pacific Northwest. Can. J. Fish. Aquat. Sci. 61, 283–291.
Leopold, L.B., 1994. A View of the River. Harvard Univ. Press, Cambridge, MA.
Leopold, L.B., Wolman, M.G., 1957. River channel patterns: braided, meandering, and straight. U.S. Geological Survey Professional Paper, vol. 282-B, pp. 39–84.
Leopold, L.B., Wolman, M.G., Miller, J.P., 1964. Fluvial Processes in Geomorphology. W.H. Freeman and Co., San Francisco, CA.
Li, R., Shen, H.W., 1973. Effect of tall vegetation on flow and sediment. J. Hydraul. Div., ASCE 99 (HY5), 793–814.
Lisle, T.E., 1982. Effects of aggradation and degradation on riffle-pool morphology in natural gravel channels, northwestern California. Water Resour. Res. 18 (6), 1643–1651.
Lisle, T.E., Nelson, J.M., Pitlick, J., Madej, M.A., Barkett, B.L., 2000. Variability of bed mobility in natural, gravel-bed channels and adjustments to sediment load at local and reach scales. Water Resour. Res. 36 (12), 3743–3755.
MacFarlane, W.A., Wohl, E., 2003. Influence of step composition of step geometry and flow resistance in step-pool streams of the Washington Cascades. Water Resour. Res. 39 (2), 1037–1049. doi:10.1029/2001WR0011238.
Mackin, J.H., 1948. Concept of the graded river. Geol. Soc. Amer. Bull. 59, 463–512.
Madej, M.A., 2001. Development of channel organization and roughness following sediment pulses in single-thread, gravel bed rivers. Water Resour. Res. 37 (8), 2259–2272.
Manga, M.M., Kirchner, J.W., 2000. Stress partitioning in streams by large woody debris. Water Resour. Res. 36 (8), 2373–2379.
Maser, C., Sedell, J.R., 1994. From the Forest to the Sea: The Ecology of Wood in Streams, Rivers, Estuaries and Oceans. St. Lucie Press, Delray Beach, FL.
Millar, R.G., 1999. Grain and form resistance in gravel-bed rivers. J. Hydraul. Res. 37 (3), 303–312.
Millar, R.G., Quick, M.C., 1994. Flow resistance of high-gradient gravel channels. In: Cotroneo, G.V., Rumer, R.R. (Eds.), Hydraulic Engineering'94, Proceedings of the 1994 Conference, vol. 1. American Society of Civil Engineers, Buffalo, NY, pp. 717–721.
Millar, R.G., Rennie, C.D., 2001. Comment on "Effects of hydraulic roughness on surface textures of gravel-bed rivers" by J.M. Buffington and D.R. Montgomery. Water. Resour. Res. 37 (5), 1527–1528.
Montgomery, D.R., Buffington, J.M., 1997. Channel-reach morphology in mountain drainage basins. Geol. Soc. Amer. Bull. 109, 596–611.
Montgomery, D.R., Panfil, M.S., Hayes, S.K., 1999. Channel-bed mobility response to extreme sediment loading at Mount Pinatubo. Geology 27 (3), 271–274.
Morisawa, M., 1968. Streams, Their Dynamics and Morphology. McGraw-Hill, New York.
Mossop, B., Bradford, M.J., 2006. Using thalweg profiling to assess and monitor juvenile salmon (*Oncorhynchus spp.*) habitat in small streams. Can. J. Fish. Aquat. Sci. 63, 1515–1525.
Mueller, E.R., Pitlick, J., Nelson, J.M., 2005. Variation in the reference Shields stress for bed load transport in gravel-bed streams and rivers. Water Resour. Res. 41, W04006. doi:10.1029/2004WR003692.
Musseter, R.A., 1989. Dynamics of mountain streams. PhD Dissertation, Department of Geosciences, Colorado State University, Fort Collins.
Nehlsen, W., Williams, J.E., Lichatowich, J.A., 1991. Pacific salmon at the crossroads: stocks at risk from California, Oregon, Idaho, and Washington. Fisheries 16 (2), 4–21.
Nelson, J.M., Smith, J.D., 1989. Flow in meandering channels with natural topography. In: Ikeda, S., Parker, G. (Eds.), River Meandering. American Geophysical Union, Washington, DC, pp. 69–102.
Olsen, D.S., Whitaker, A.C., Potts, D.F., 1997. Assessing stream channel stability thresholds using flow competence estimates at bankfull stage. J. Am. Water Resour. Assoc. 33 (6), 1197–1207.
Omernik, J.M., 1987. Ecoregions of the conterminous United States, map scale 1:7,500,000. Ann. Assoc. Am. Geogr. 77 (1), 118–125.
Parker, G.P., Toro-Escobar, C.M., Ramey, M., Beck, S., 2003. Effect of floodwater extraction on mountain stream morphology. J. Hydraul. Eng. ASCE 129 (11), 885–895. doi:10.1061/(ASCE)0733–9429(2003)129:11(885).
Peck, D.V., Herlihy, A.T., Hill, B.H., Hughes, R.M., Kaufmann, P.R., Klemm, D.J., Lazorchak, J.M., McCormick, F.H., Peterson, S.A., Ringold, P.L., Magee, T., Cappaert, M., 2006. Environmental Monitoring and Assessment Program-Surface Waters Western Pilot Study: Field Operations Manual for Wadeable Streams. EPA/620/R-06/003. U.S. Environmental Protection Agency, Office of Research and Development, Washington, DC.
Petryk, S., Bosmajian III, G., 1975. Analysis of flow through vegetation. J. Hydraul. Div., ASCE 101, 871–884.
Paola, C., Mohrig, D., 1996. Paleohydraulics revisited: palaeoslope estimation in coarse-grained braided rivers. Basin Res. 8, 243–254.
Robison, E.G., Beschta, R.L., 1989. Estimating stream cross sectional area from wetted width and thalweg depth. Phys. Geogr. 10 (2), 190–198.
Robison, E.G., Kaufmann, P.R., 1994. Evaluating two objective techniques to define pools in small streams. In: Marston, R.A., Hasfurther, V.A. (Eds.), Effects of Human Induced Changes on Hydrologic Systems. Summer Symposium Proceedings, American Water Resources Association, June 26–29, 1994. Jackson Hole, WY, pp. 659–668.
Sabol, G.V., Nordin Jr., C.F., 1978. Dispersion in rivers as related to storage zones. J. Hydraul. Div., ASCE 104 (HY5), 695–708.
Schumm, S.A., 1971. Fluvial geomorphology: channel adjustment and river metamorphosis. In: Shen, H.W. (Ed.), River Mechanics, vol. I. Fort Collins, CO, pp. 5–1–5–22.
Shields, A., 1936. Anwendung der Aehnlichkeitsmechanik und der turbulenzforschung auf die geschiebebewegung. Mitt. Preuss. Versuchsanst. Wasserbau Schiffbau, vol. 26. Berlin, Germany. As cited in Parker et al., 2003.

Shields, F.D., Gippel, C.J., 1995. Prediction of effects of woody debris removal on flow resistance. J. Hydraul. Eng., ASCE 121, 341–354.

Shields, F.D., Smith, R.H., 1992. Effects of large woody debris removal on physical characteristics of a sand-bed river. Aquat. Conserv.: Mar. Freshw. Ecosyst. 2, 145–163.

Spence, B.C., Lomnicky, G.A., Hughes, R.M., Novitzki, R.P., 1996. An ecosystem approach to salmonid conservation. National Marine Fisheries Service, Report TR-4501–96–6057, Portland, Oregon.

Stevens, D.L., Olsen, A.R., 1999. Spatially restricted surveys over time for aquatic resources. J. Agric. Biol. Environ. Stat. 4 (4), 415–428.

Stevens, D.L., Olsen, A.R., 2004. Spatially-balanced sampling of natural resources. J. Am. Stat. Assoc. 99 (465), 262–278.

Stoddard, J.L., Peck, D.V., Paulsen, S.G., Van Sickle, J., Hawkins, C.P., Herlihy, A.T., Hughes, R.M., Kaufmann, P.R., Larsen, D.P., Lomnicky, G., Olsen, A.R., Peterson, S.A., Ringold, P.L., Whittier, T.R., 2005a. An Ecological Assessment of Western Streams and Rivers. EPA 620/R-05/005. U.S. Environmental Protection Agency, Washington, DC.

Stoddard, J.L., Peck, D.V., Olsen, A.R., Larsen, D.P., Van Sickle, J., Hawkins, C.P., Hughes, R.M., Whittier, T.R., Lomnicky, G., Herlihy, A.T., Kaufmann, P.R., Peterson, S.A., Ringold, P.L., Paulsen, S.G., Blair, R., 2005b. Environmental Monitoring and Assessment Program Western Streams and Rivers Statistical Summary. EPA 620/R-05/006. U.S. Environmental Protection Agency, Washington, DC.

Strahler, A.N., 1957. Quantitative analysis of watershed geomorphology. Trans. Am. Geophys. Union 38, 913–920.

TIGER, 1990. http://www.census.gov/geo/www/tiger1990.

Trimble, S.W., 1999. Decreased rates of alluvial sediment storage in the Coon Creek basin, Wisconsin, 1975–93. Science 285, 1244–1246.

Waters, T.F., 1995. Sediment in Streams – Sources, Biological Effects, and Control. Monogr. Am. Fish. Soc. Symp., vol. 7. Bethesda, MD.

Wiberg, P.L., Smith, J.D., 1991. Velocity distribution and bed roughness in high-gradient streams. Water Resour. Res. 27, 825–838.

Wilcock, P.R., 1997. The components of fractional transport rate. Water Resour. Res. 33 (1), 247–258.

Wilcock, P.R., 1998. Two-fraction model of initial sediment motion in gravel-bed rivers. Science 280, 410–412.

Wilcock, P.R., 2001. Comment on "Effects of hydraulic roughness on surface textures of gravel-bed rivers" by J.M. Buffington and D.R. Montgomery. Water Resour. Res. 37 (5), 1525–1526.

Wilcox, A.C., Wohl, E.E., 2006. Flow resistance dynamics in step-pool stream channels: 1. Large woody debris and controls on total resistance. Water Resour. Res. 42, W05418. doi:10.1029/2005WR004277.

Wilcox, A.C., Nelson, J.M., Wohl, E.E., 2006. Flow resistance in step-pool channels: 2. Partitioning between grain, spill, and woody debris resistance. Water Resour. Res. 42, W05419. doi:10.1029/2005WR004278.

Wohl, E., Merritt, D., 2005. Prediction of mountain stream morphology. Water Resour. Res. 41, W08419.

Wolman, M.G., 1954. A method of sampling coarse river-bed material. Trans. Am. Geophys. Union 35 (6), 951–956.

Wolman, M.G., 1955. The natural channel of Brandywine Creek Pennsylvania. U.S. Geological Survey Professional Paper, vol. 271. 56 pp.

Wolman, M.G., Miller, J.P., 1960. Magnitude and frequency of forces in geomorphic processes. J. Geol. 68, 54–74.

Wu, W., Shields Jr., F.D., Bennett, S.J., Wang, S.S.Y., 2005. A depth-averaged two-dimensional model for flow, sediment transport, and bed topography in curved channels with riparian vegetation. Water Resour. Res. 41, W03015. doi:10.1029/2004WR003730.

Yalin, M.S., Karahan, E., 1979. Inception of sediment transport. J. Hydraul. Div., ASCE 105 (HY-11), 1433–1443.